

# UNCOVERING MESA-OPTIMIZATION ALGORITHMS IN TRANSFORMERS

**Johannes von Oswald**\*,<sup>1</sup>  
ETH Zürich &  
Google Research

**Eyvind Niklasson**\*  
Google Research

**Maximilian Schlegel**\*  
ETH Zürich

**Seijin Kobayashi**  
ETH Zürich

**Nicolas Zucchet**  
ETH Zürich

**Nino Scherrer**  
Independent Researcher

**Nolan Miller**  
Google Research

**Mark Sandler**  
Google Research

**Blaise Agüera y Arcas**  
Google Research

**Max Vladymyrov**  
Google Research

**Razvan Pascanu**  
Google DeepMind

**João Sacramento**<sup>1</sup>  
ETH Zürich

## ABSTRACT

Transformers have become the dominant model in deep learning, but the reason for their superior performance is poorly understood. Here, we hypothesize that the strong performance of Transformers stems from an architectural bias towards mesa-optimization, a learned process running within the forward pass of a model consisting of the following two steps: (i) the construction of an internal learning objective, and (ii) its corresponding solution found through optimization. To test this hypothesis, we reverse-engineer a series of autoregressive Transformers trained on simple sequence modeling tasks, uncovering underlying gradient-based mesa-optimization algorithms driving the generation of predictions. Moreover, we show that the learned forward-pass optimization algorithm can be immediately repurposed to solve supervised few-shot tasks, suggesting that mesa-optimization might underlie the in-context learning capabilities of large language models. Finally, we propose a novel self-attention layer, the mesa-layer, that explicitly and efficiently solves optimization problems specified in context. We find that this layer can lead to improved performance in synthetic and preliminary language modeling experiments, adding weight to our hypothesis that mesa-optimization is an important operation hidden within the weights of trained Transformers.

## 1 INTRODUCTION

Transformers (Vaswani et al., 2017) and especially large language models (LLMs) are known to strongly adjust their predictions and learn based on data given in-context (Brown et al., 2020). Recently, a number of works have studied this phenomenon in detail by meta-learning Transformers to solve few-shot tasks, providing labeled training sets in context. These studies discovered that Transformers implement learning algorithms that either closely resemble or exactly correspond to gradient-based optimizers (Garg et al., 2022; Akyürek et al., 2023; von Oswald et al., 2023; Kirsch et al., 2022; Zhang et al., 2023; Mahankali et al., 2023; Ahn et al., 2023; Li et al., 2023a).

However, it remains unclear how well these findings on meta-trained Transformers translate to models that are *autoregressively-trained* on sequential data, the prevalent LLM training setup. Here, we address this question by building on the theoretical construction of von Oswald et al. (2023), and show how Transformers trained on sequence modeling tasks predict using gradient-descent learning based on in-context data. Thus, we demonstrate that minimizing a generic autoregressive loss gives rise to a subsidiary gradient-based optimization algorithm running inside the forward pass of a Transformer. This phenomenon has been recently termed mesa-optimization (Hubinger et al., 2019). Moreover, we find that the resulting mesa-optimization algorithms exhibit in-context few-shot learning capabilities, independently of model scale. Our results therefore complement previous reports characterizing the emergence of few-shot learning in large-scale LLMs (Kaplan et al., 2020; Brown et al., 2020).

\*These authors contributed equally to this work. <sup>1</sup>Correspondence to jvoswald@google.com, rjoao@ethz.ch.

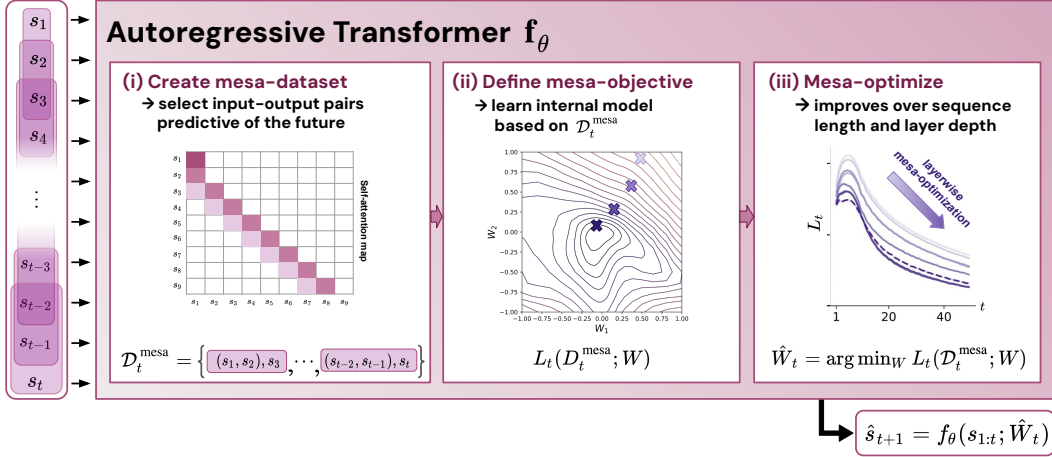


Figure 1: **Illustration of our hypothesis:** Optimizing the weights  $\theta$  of an autoregressive Transformer  $f_\theta$  gives rise to mesa-optimization algorithms implemented in the forward pass of the model. As a sequence of inputs  $s_1, \dots, s_t$  is processed up to timestep  $t$ , the Transformer (i) creates an internal training set consisting of pairs of input-target associations, (ii) defines an internal objective function through the resulting dataset, used to measure the performance of an internal model with weights  $W$ , (iii) optimizes this objective and uses the learned model to generate a prediction  $\hat{s}_{t+1}$  of the future.

Our contributions are as follows:

- We generalize the construction of von Oswald et al. (2023) and show how, in theory, Transformers can autoregressively predict the next element of a sequence by optimizing internally-constructed objectives with gradient-based methods.
- Experimentally, we reverse-engineer Transformers trained on simple sequence modeling tasks, and find strong evidence that their forward pass implements two-step algorithms: (i) early self-attention layers construct internal training datasets by grouping and copying tokens, and therefore implicitly define internal objective functions, (ii) deeper layers optimize these objectives to generate predictions.
- Similarly to LLMs, we show that these simple autoregressively-trained models become in-context learners, and that prompt-tuning, crucial to improve in-context learning in LLMs, also improves performance in our setting.
- Motivated by our findings that attention layers are attempting to implicitly optimize internal objective functions, we introduce the *mesa-layer*, a novel attention layer that efficiently solves a least-squares optimization problem, instead of taking just a single gradient step towards an optimum. We show that a single mesa-layer outperforms deep linear and softmax self-attention Transformers on simple sequential tasks while offering more interpretability.
- We carry out preliminary language modeling experiments replacing standard self-attention layers with the mesa-layer, and obtain promising results demonstrating strong in-context learning capabilities enabled by the layer.

## 2 PRELIMINARIES

**Self-attention.** We study causally-masked, autoregressive Transformers (Vaswani et al., 2017) where self-attention (Bahdanau et al., 2015) is the elementary building block. Given a sequence of  $t$  input tokens  $E_t = (e_{t'})_{t'=1}^t$ , representing the first  $t$  time steps, a self-attention layer with  $H$  heads and parameters  $\theta$  updates the current token  $e_t \in \mathbb{R}^{D_e}$  as follows:

$$\Delta e_t^{\text{softmax}}(E_t, \theta) = \sum_{h=1}^H P_h V_{h,t} \text{softmax}(K_{h,t}^\top q_{h,t}), \quad (1)$$

where  $q_{h,t} = W_{h,q} e_t \in \mathbb{R}^{D_a}$  is referred to as a query, each column  $k_{h,t'} = W_{h,k} e_{t'} \in \mathbb{R}^{D_a}$  of matrix  $K_{h,t} \in \mathbb{R}^{D_a \times t}$  as a key, and each column  $v_{h,t'} = W_{h,v} e_{t'} \in \mathbb{R}^{D_v}$  of matrix  $V_{h,t} \in \mathbb{R}^{D_v \times t}$  as a value. The nonlinear function  $\text{softmax}(a)$  applied to vector  $a \in \mathbb{R}^t$  returns an attention vector with entries  $[\text{softmax}(a)]_i = \frac{\exp(a_i)}{\sum_{t'=1}^t \exp(a_{t'})}$ . We absorb bias terms and assume here for

conciseness that all heads are equally sized. The parameters  $\theta$  of this layer are the projection matrices  $\{(P_h, W_{h,q}, W_{h,k}, W_{h,v})\}_{h=1}^H$  for all heads. Transformers include other layers that we do not review here, notably multi-layer perceptrons (MLPs) and layer normalization (LayerNorm) units.

We also consider linear attention models (e.g., Katharopoulos et al., 2020; Wang et al., 2020; Schlag et al., 2021; Choromanski et al., 2021), which simply omit the softmax nonlinearity:

$$\Delta e_t^{\text{linear}}(E_t, \theta) = \sum_{h=1}^H P_h V_{h,t} K_{h,t}^\top q_{h,t} = \sum_{h=1}^H P_h \hat{W}_{h,t}^{\text{linear}} q_{h,t}. \quad (2)$$

Above, we rewrite this equation using a weight matrix  $\hat{W}_{h,t}^{\text{linear}} = \sum_{t'=1}^t v_{h,t'} k_{h,t'}^\top$ . The size of this weight matrix does not scale with time, but it encodes information from all past tokens  $(e_{t'})_{t'=1}^t$ , allowing inference at constant memory cost. For this reason, there is at present considerable interest in linear attention (Fournier et al., 2023; Treviso et al., 2023).

**Linear self-attention can implement one step of gradient descent.** Our starting point is the main result of von Oswald et al. (2023), who showed that one such attention layer can implement one step of gradient descent (GD) on a quadratic cost function evaluated on in-context data. Therefore, multi-layer Transformers can, in theory, minimize the loss down to an arbitrary desired level through multiple steps of GD. In this paper, we extend this result to the autoregressive setting. First, we review the original model and task setting.

In the setup of von Oswald et al. (2023), the goal is to meta-learn the parameters  $\theta$  of a linear self-attention layer such that it learns to solve supervised learning tasks, similarly to related work (Garg et al., 2022; Akyürek et al., 2023; Kirsch et al., 2022; Zhang et al., 2023; Mahankali et al., 2023; Ahn et al., 2023; Li et al., 2023a). Each task  $\tau$  is specified in-context by a training set  $\mathcal{D}_\tau = \{(x_{\tau,i}, y_{\tau,i})\}_{i=1}^N$  and a test input  $x_{\tau,\text{test}}$ . The goal of meta-learning is then  $\min_\theta \mathbb{E}_\tau [\|y_{\tau,\text{test}} - f(x_{\tau,\text{test}}, \mathcal{D}_\tau, \theta)\|^2]$ , where  $y_{\tau,\text{test}}$  is the correct output revealed during meta-learning,  $f(x_{\tau,\text{test}}, \mathcal{D}_\tau, \theta)$  denotes the actual output of the linear self-attention layer, and the expectation is taken over a distribution of linear regression tasks.

A standard approach for solving a linear regression task is to resort to a linear model  $f_W(x) = Wx$  with parameters  $W \in \mathbb{R}^{D_y \times D_x}$  learned by gradient descent on the squared error loss  $L(W, \mathcal{D}_\tau) = \sum_{i=1}^N \frac{1}{2} \|y_{\tau,i} - f_W(x_{\tau,i})\|^2$ . Starting from an initial parameter  $W_0$ , a gradient-descent learner updates it by taking a step  $\Delta W_0$  of size  $\eta$  along the negative of the gradient,  $\nabla L = \sum_{i=1}^N (y_{\tau,i} - W_0 x_{\tau,i}) x_{\tau,i}^\top$ . The main result of von Oswald et al. (2023) is a theoretical construction showing that a linear self-attention layer can implement exactly one such gradient descent step. We briefly sketch this result now.

First, we construct a set of tokens  $E_T$ , with  $T = N$ , such that  $e_t = (y_{\tau,i}, x_{\tau,i})$ , with  $y_{\tau,i}$  and  $x_{\tau,i}$  concatenated. Additionally, we create a query token  $e_{T+1} = (-W_0 x_{\tau,\text{test}}, x_{\tau,\text{test}})$  not contained within the set  $\mathcal{D}_\tau$ , where we place the test input for which a prediction should be made. Under this token construction and using the symbol  $I_x$  to denote the identity matrix of size  $\dim(x)$ , if all bias terms are zero and  $W_k^\top W_q = \begin{pmatrix} 0 & 0 \\ 0 & I_x \end{pmatrix}$ , and  $PW_v = \begin{pmatrix} -\eta I_y & \eta W_0 \\ 0 & 0 \end{pmatrix}$ , the query token  $e_{T+1}$ , after one such layer, becomes  $-(W_0 + \Delta W_0)x_{\tau,\text{test}}, x_{\tau,\text{test}}$ . The  $y$ -component of this token contains the (negative) of the prediction obtained by a linear model that underwent one step ( $\Delta W_0$ ) of gradient descent. Therefore, this self-attention layer implicitly constructs a least-squares optimization problem and takes one step of *mesa-gradient descent* towards solving it. This layer can be directly stacked to implement multiple steps of GD, cf. Appendix A4.2. The term *mesa* reinforces that this optimization occurs within the forward attention dynamics, without any actual change to the parameters of the attention layer itself (Hubinger et al., 2019). We stress the necessary assumption of having  $x_{\tau,i}$  and  $y_{\tau,i}$  concatenated within a single token.

### 3 SEQUENTIAL PREDICTION BY LEAST-SQUARES MESA-OPTIMIZATION

The construction reviewed above is designed to solve few-shot supervised learning problems. As we see next, moving to a general autoregressive modeling setting requires minimal change. However, the spirit of what follows is markedly different: we no longer ask whether an attention layer can

solve few-shot supervised learning problems that are presented in-context. Instead, we ask whether Transformers can rely on mesa-gradient descent to predict future inputs.

We therefore move to the case where a self-attention layer has to learn sequentially as some inputs  $s_{1:T}$  are gradually unveiled. The goal at time  $t$  is now to minimize the autoregressive loss:

$$L_t(W) = \sum_{t'=1}^{t-1} \frac{1}{2} \|s_{t'+1} - W s_{t'}\|^2, \quad (3)$$

where  $s_{t'+1}$  serves as the label for  $s_{t'}$ . As in the previous section, we assume that the model always starts from the same initial weights  $W_0$ , and that learning corresponds to taking only a single gradient step; this appears sub-optimal. We address this concern in the next section.

As is usually done in autoregressive modeling we apply causal masking, and at time  $t$  we update token  $e_t$  using the in-context data available in  $E_t$ . To adapt to the autoregressive setting, we adapt the token construction to a three-channel code,  $e_t = (-W_0 s_t, s_t, s_{t-1})$ , to include an additional separate first channel to be filled with the prediction  $\hat{s}_{t+1}$  of future inputs at every time step  $t$ , alongside channels for the previous and current sequence element, with the latter playing the role of target in the construction of von Oswald et al. (2023). Note that by providing neighboring elements  $s_t, s_{t-1}$  within one token  $e_t$ , self-attention is able to compute dot products of *targets* and *inputs* of the loss  $L_t(W)$  necessary to compute  $\nabla L_t$ , see Eq. 3. Then, to update the first channel of such a token with the prediction of a linear model learned with one step of gradient descent, it suffices to set

$$PW_v = \begin{pmatrix} 0 & -\eta I_s & \eta W_0 \\ 0 & 0 & 0 \\ 0 & 0 & 0 \end{pmatrix}, \quad \text{and} \quad W_k^\top W_q = \begin{pmatrix} 0 & 0 & 0 \\ 0 & 0 & 0 \\ 0 & I_s & 0 \end{pmatrix}. \quad (4)$$

We refer to this result (Eq. 4) as the one-step mesa-gradient descent construction.

**Multi-layer mesa-optimizers.** We next move to the case of deep networks comprising stacked linear self-attention layers. While it is natural to hypothesize that  $K$  layers simply implement  $K$  steps of mesa-gradient descent, as in the few-shot learning (non-autoregressive) case reviewed above, this picture might be too simple to explain actual trained autoregressive Transformers. A first hint towards this view being too narrow lies in the fact that stacking the one-step mesa-gradient descent construction (Eq. 4) over multiple layers does not yield vanilla gradient descent, as explained in Appendix A4.2. Instead, we obtain an unconventional online gradient-based optimizer, that is expected to behave worse than vanilla gradient descent. This observation, together with a mathematical analysis of the resulting optimization algorithm, can be found in a study arguing for the disadvantages of causally-masked attention for few-shot in-context learning (Ding et al., 2023). One may thus wonder if Transformers can implement more efficient mesa-optimizers.

Here, we provide an alternative mesa-optimizer that is also based on causally-masked self-attention layers. The novel optimizer operates in two stages. In a first stage, comprising one or more self-attention layers, the algorithm implements an iterative preconditioning procedure. The result of this stage is a regularized mesa-objective  $\bar{L}_t(W) = \sum_{t'=1}^{t-1} \frac{1}{2} \|s_{t'+1} - W H_t s_{t'}\|^2 + \frac{1}{2\lambda} \|W\|_F^2$ , with improved condition number compared to  $L_t(W)$ . Above,  $H_t$  is a preconditioning matrix and the scalar  $\lambda^{-1} \geq 0$  controls the regularization strength. This preconditioning procedure has the property that in the many-layer limit and under some mild conditions,  $H_t$  converges to  $H_t^* = (S_{t-1} S_{t-1}^\top + 1/\lambda I)^{-1}$ , with  $S_t$  the data matrix whose columns are  $(s_{t'})_{t'=1}^t$ . In a second stage, a final self-attention layer takes a single gradient descent step on the preconditioned mesa-objective  $\bar{L}_t(W)$ .

The two-stage algorithm described here is theoretically justified: when  $H_t = H_t^*$ , the regression problem is solved in a single step, starting from a zero-weight initialization  $W_0 = 0$ . In Appendix A4.2, we provide a simple weight and input token construction to implement this algorithm. Our novel construction leverages the truncated Neumann series to iteratively approximate the required inverse-matrix-vector products  $H_{t-1}^* s_t$  in parallel for all  $t = 2, \dots, T$ , and compactly, without ever explicitly representing any of the  $H_t$  matrices.

In Section 5 we show empirically that training a Transformer on autoregressive tasks can lead to the solutions presented above. But first, in the next section, we assume that mesa-optimization is a desirable feature for a model to have, and we discuss an architectural modification that makes this behavior built-in by default within a Transformer.

#### 4 AN ATTENTION LAYER FOR OPTIMAL LEAST-SQUARES LEARNING

Here we introduce the *mesa-layer*: a novel self-attention layer that fully solves a layer-specific optimization problem, such as the minimization of Eq. 3, instead of only descending a loss function with a single gradient step. The layer we propose is closely related to the Delta-Net model of Schlag et al. (2021), which is hardwired to do one gradient descent step per time point. We focus on causally-masked autoregressive problems, while noting that the insights remain the same for other strategies such as BERT-style masking (Devlin et al., 2019).

Given again a sequence of tokens  $E_t$ , we design a layer that changes the tokens following the update

$$\Delta e_t^{\text{mesa}}(E_t, \theta) = \sum_{h=1}^H P_h \hat{W}_{h,t}^{\text{mesa}} q_{h,t}, \quad (5)$$

$$\text{with } \hat{W}_{h,t}^{\text{mesa}} = \arg \min_W \left\{ \frac{1}{2} \sum_{t'=1}^t \|v_{h,t'} - W k_{h,t'}\|^2 + \frac{1}{2\lambda_h} \|W\|_F^2 \right\}. \quad (6)$$

Above, the scalar  $\lambda_h^{-1} > 0$  controls the strength of a regularizer added to improve generalization, and key, value and query vectors are the usual learned head-specific affine transformations of the tokens, as before. However, through Eq. 6 these vectors are now assigned a precise, interpretable role: value vectors specify targets to which an internal model with parameters  $W$  should map training and test inputs, represented by keys and queries, respectively. The minimizer of a regularized version of Eq. 3 can be immediately mapped to Eq. 6 under the token construction discussed in Section 3 by appropriately setting the projection matrices  $W_{h,v}$ ,  $W_{h,k}$  and  $W_{h,q}$ .

At any given time step  $t = 1, \dots, T$  computing  $\Delta e_t^{\text{mesa}}$  requires solving a regularized least squares problem per head. To efficiently solve this sequence of  $T$  optimization problems, we will leverage the recursive dependency of the solutions of these consecutive problems which can be expressed in closed-form as

$$\hat{W}_{h,t}^{\text{mesa}} = V_{h,t} K_{h,t}^\top R_{h,t} = \sum_{t'=1}^t v_{h,t'} k_{h,t'}^\top \left( \sum_{t'=1}^t k_{h,t'} k_{h,t'}^\top + 1/\lambda_h I \right)^{-1}. \quad (7)$$

Note that if we drop the inverted matrix  $R_{h,t}$ , we recover a standard linear self-attention layer, cf. Eq. 2. A recent study has also shown that the solution of a least-squares problem can be expressed as a generalized attention layer (Garnelo & Czarnecki, 2023).

We now use the Sherman & Morrison (1950) formula to obtain the inverse at time  $t$  from the inverse at the previous time step  $t - 1$ . This iterative update is possible because we only change the inverse by a rank-one update. This solution scheme is known as recursive least squares (Gauss, 1821). We obtain through Sherman-Morrison the recursion

$$R_{h,t} = R_{h,t-1} - \frac{R_{h,t-1} k_{h,t} k_{h,t}^\top R_{h,t-1}}{1 + k_{h,t}^\top R_{h,t-1} k_{h,t}} \quad (8)$$

with  $R_{h,0} = \lambda_h I$ . With this, we can (causally in time) compute

$$\Delta e_t^{\text{mesa}}(E_t, \theta) = \sum_{h=1}^H P_h V_{h,t} K_{h,t}^\top R_{h,t} q_{h,t} \quad (9)$$

which requires 2 additional vector-matrix and 2 vector-vector multiplications per step compared to the standard self-attention operation. Note that since our intermediates consist of matrices of dimension  $D_a \times D_a$  across the timesteps, naive backward gradient computation requires storing them in memory. Fortunately, this memory overhead can be avoided using the Sherman-Morrison formula in reverse during the backward pass, cf. Appendix A2.1, enabling memory-efficient gradient computation of the output of the mesa-layer w.r.t. its inputs. We further note that while the implementation described here has a desirable  $\mathcal{O}(1)$  inference memory cost like standard linear self-attention, it is not parallelizable across time during training. This is a disadvantage for training on contemporary hardware shared with recurrent neural networks, but not with standard softmax or linear self-attention. As discussed in Appendix A2.1, in practice this significantly slows down our experiments.

We demonstrate the expressivity and performance of the mesa-layer in reverse-engineerable sequence learning tasks as well as in language modeling in the next sections.

## 5 EMPIRICAL ANALYSIS

### 5.1 PREDICTION OF LINEAR DYNAMICS BY IN-CONTEXT LEARNING

We now attempt to reverse-engineer Transformers trained on simple synthetic autoregressive tasks. We have two main goals. First, we want to understand whether autoregressively-trained Transformers use mesa-optimization algorithms to predict future inputs. We use the constructions presented in Section 3 to guide our reverse-engineering analyses. Our second goal is to determine if introducing the mesa-layer improves the performance of standard Transformers, by subsuming multiple attention layers that are otherwise needed to go beyond one mesa-gradient descent step.

**Generative model.** We focus on fully-observed linear dynamical systems. For all experiments described in this section, we use the following generative model. To create a sequence  $s_{1:T}$  we first draw a random groundtruth  $D_s \times D_s$  weight matrix  $W^*$  as well as a random initial state  $s_1 \sim \mathcal{N}(0, I_s)$ ; subsequent states for  $t = 2, \dots, T$  are then generated according to the rule  $s_{t+1} = W^* s_t + \epsilon_t$ , where  $\epsilon_t \sim \mathcal{N}(0, \sigma_s^2 I_s)$  introduces Gaussian noise. We take  $W^*$  to be a random orthogonal matrix<sup>1</sup>. The generation of  $W^*$  anew for each sequence avoids the memorization solution that stores  $W^*$  in  $\theta$ , and corresponds to a highly simplified toy model meant to capture the diversity present in real-world data. A similar in spirit design choice may be found in the hierarchical generative model of Xie et al. (2022). We refer to Appendix A6.1 for additional experimental details. Under such an assumed groundtruth dynamics, the standard way of predicting future states from a given past sequence  $s_{1:t}$  is to use a linear model,  $s_{t+1} = W s_t$ , where the weights  $W$  are learned by minimizing  $L_t(W)$ , Eq. 3, possibly with an added regularizer.

**Training and in-context learning objectives.** Here, we analyze various configurations of Transformers trained through stochastic online minimization of the autoregressive loss

$$\mathcal{L}(\theta) = \mathbb{E}_s \left[ \sum_{t=1}^{T-1} \mathcal{L}_t(s_{1:t}, \theta) \right] = \mathbb{E}_s \left[ \frac{1}{2} \sum_{t=1}^{T-1} \|s_{t+1} - f_t(s_{1:t}, \theta)\|^2 \right], \quad (10)$$

where the expectation is taken under the sequence distribution described above,  $f_t(s_{1:t}, \theta)$  denotes the output of the Transformer model using  $s_t$  as query and  $s_{1:t}$  as context, and  $\theta$  are the Transformer parameters, which vary depending on the exact architecture being trained. To avoid confusion with mesa-optimization, we refer to the minimization of  $\mathcal{L}(\theta)$  as the base-optimization process.

Here and throughout, to measure in-context learning performance we take the per-timestep loss  $\mathcal{L}_t(s_{1:t}, \theta)$  and monitor its evolution as a function of context size  $t$ . Thus, we simply measure how future-input predictions improve as more context is provided to the model. This corresponds to the operational definition of in-context learning proposed by Kaplan et al. (2020).

**Hypothesis statement.** The hypothesis we pursue is that base-optimization of  $\mathcal{L}(\theta)$  gives rise to a mesa-optimization process in charge of generating predictions  $f_t(s_{1:t}, \theta)$ , as illustrated in Figure 2A. More concretely, for our linear generative model, we hypothesize that learning yields Transformers that predict future inputs by implicitly, and entirely within their forward dynamics: (i) representing a linear model with mesa-parameters  $W$ , (ii) constructing the least-squares mesa-objective  $L_t(W)$ , cf. Eq. 3, using in-context data  $s_{1:t}$ , (iii) learning  $W$  by minimizing the mesa-objective, and (iv) applying  $W$  to predict the next token  $s_{t+1}$ . We note that, according to our hypothesis, the mesa-objective  $L_t(W)$  governing the forward pass of our Transformer coincides with the base-objective  $\mathcal{L}(\theta)$ , but now defined w.r.t. an implicit linear autoregressive model with mesa-parameters  $W$ .

**Single self-attention layer.** We begin by verifying our hypothesis on single-layer, linear-attention-only Transformers, using the token construction of Section 3,  $e_t = (0, s_t, s_{t-1})$ . We hypothesize that feeding the Transformer with input-target pairs provides an inductive bias towards mesa-gradient descent. Using this token construction, we then train by online mini-batch gradient descent on  $\mathcal{L}(\theta)$ , generating new sequences at each base optimization step according to the process described above.

<sup>1</sup>This detail turns out to be important; we found that converging linear dynamics led to different inference algorithms. We discuss this point in Appendix A5.

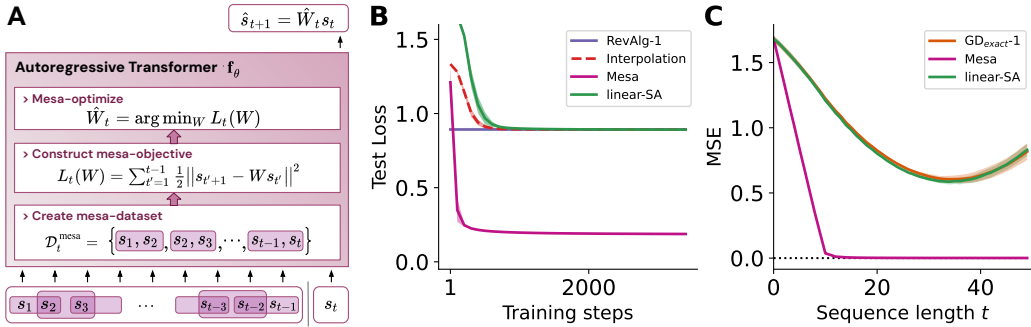


Figure 2: **Reverse-engineering a trained linear self-attention layer.** (A) Transformers mesa-optimize an internal linear model and use it to predict the future state of a linear dynamical system. (B) A trained 2-head linear self-attention layer (linear-SA) is perfectly described by a reverse-engineered mesa-gradient descent algorithm (RevAlg-1; see Eq. A43). We show also the performance achieved by an interpolation model, obtained by averaging the parameters  $\theta$  of the trained model and those expected from our reverse-engineered construction. (C) In-context learning loss after training: next-input  $s_{t+1}$  mean squared prediction error (MSE) as a function of sequence length. The trained linear-SA layer is very well described by a linear model learned by one step of gradient descent with a tuned learning rate ( $\text{GD}_{\text{exact-1}}$ ). Linear-SA is greatly outperformed by a single mesa-layer, which optimally solves the autoregressive learning problem at every time point  $t$ , reaching minimal mean-squared prediction error after observing enough examples. By contrast, one-step GD runs into capacity issues, exhibiting non-monotonic MSE as a function of sequence length. Averages over 5 different seeds; shaded area represents standard deviation.

We are able to perfectly identify the algorithm (RevAlg-1) that this single-layer Transformer uses to generate predictions. Visual inspection of the projection matrices is revealing, cf. Figure A2: we see that the dominant pattern coincides with our one-step mesa-gradient descent construction, Eq. 4, plus some identification noise. We verify quantitatively that the layer is indeed implementing a step of mesa-gradient descent by (i) comparing the loss reached by the trained layer with a linear autoregressive model learned through one step of gradient descent, and by (ii) studying an interpolated model, obtained by averaging directly in parameter space learned and constructed weights, cf. Appendix A6.1. We find that we can perfectly fit our trained layer when using all degrees of freedom in our construction, including not only a learned learning rate  $\eta$ , but also a learned set of initial weights  $W_0$ , reminiscent of the model-agnostic meta-learning method of Finn et al. (2017).

Importantly, as shown in Figure 2, the resulting learned one-step algorithm is still vastly outperformed by a single mesa-layer. We note that under a simple setting of its weights, easily discovered by base-optimization, this layer can optimally solve the task studied here. This result demonstrates the advantage of hardcoded inductive biases in favor of mesa-optimization.

**Multiple self-attention layers.** Armed with our theoretical insights for the multi-layer case, cf. Section 3, we now analyze deep linear and softmax attention-only Transformers. We format our inputs according to a 4-channel construction,  $e_t = (0, s_t, s_t, s_{t-1})$ , which corresponds to choosing  $W_0 = 0$ . This makes it possible to implement both multi-step mesa-optimization and our iterative preconditioning algorithm, as well as hybrid variants mixing both, as discussed in Appendix A4.2.

Like with single-layer models, we see clean structure in the weights of the trained models, see Figures A7 and A5. As a first reverse-engineering analysis, we exploit this structure and construct an algorithm (RevAlg- $d$ , where  $d$  denotes layer number) comprising 16 parameters (instead of 3200) per layer head. We find that this compressed, albeit convoluted, expression can describe a trained model. In particular, it allows interpolating between actual Transformer and RevAlg- $d$  weights in an almost lossless fashion, cf. Figure 3A. Experimental details can be found in Appendix A6.1.2.

While the RevAlg- $d$  expression explains a trained multi-layer Transformer with a small number of free parameters, it is difficult to interpret it as a mesa-optimization algorithm. We, therefore, resort to a linear regression probing analysis (Alain & Bengio, 2017; Akyürek et al., 2023) to look for signatures of our hypothesized mesa-optimization algorithms. In particular, we seek evidence both for the stacked multi-layer gradient descent construction, which should bring the outputs of intermediate

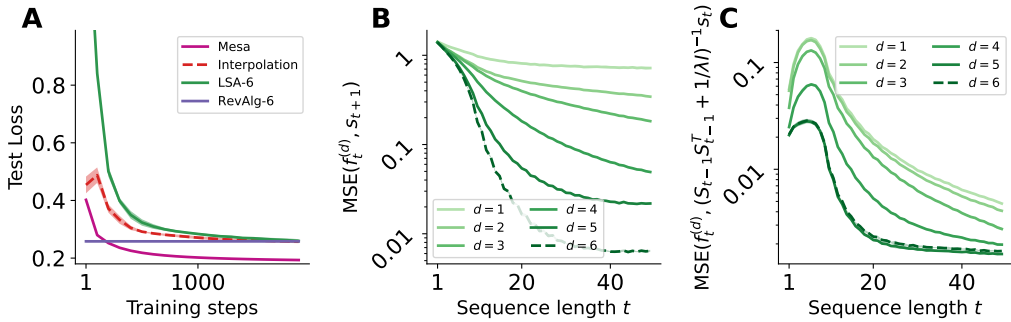


**Figure 3: Reverse-engineering multi-layer Transformers trained on constructed token inputs.** We report results for a 6-layer linear-self-attention-only Transformer. (A) As training proceeds, this multi-layer linear model (LSA-6) is again perfectly described by a reverse-engineered algorithm (RevAlg-6), described in Appendix A4. Note that the model is still outperformed by a single trained mesa-layer. (B & C) We linearly regress the activations of each layer against (B) final targets (target probing) as well as (C) the preconditioned inputs  $(S_{t-1}S_{t-1}^T + 1/\lambda I)^{-1}s_t$  predicted by our theory (inverse probing), observing an improvement in linear decoding performance across layers. Averages computed over 5 different seeds; shaded area represents standard deviation.

layers closer to the desired targets; and for our novel iterative preconditioning algorithm, which should bring layer outputs closer to  $H_t^* s_t$ . We therefore carry out our probing analysis taking as targets for regression (i) the future state to be predicted  $s_{t+1}$  used as the target to train the Transformer, which we term the *target probe*; and (ii) the preconditioned current input,  $(S_{t-1}S_{t-1}^T + 1/\lambda I)^{-1}s_t$ , which we term the *inverse probe*, and that would allow for solving the least-squares problem in a single gradient descent step as discussed above. Experimental details on how exactly we carry out these regression analyses can be found in Appendix A6.1.2.

As shown in Figure 3 for deep linear self-attention Transformers (see Figure A14 for a softmax model) we see that *both* probes can be linearly decoded, with decoding performance increasing with sequence length and network depth. Base-optimization has therefore discovered a hybrid algorithm that descends over layers the original mesa-objective  $L_t(W)$  while simultaneously improving the condition number of the mesa-optimization problem. This leads to a fast descent of the mesa-objective  $L_t(W)$ , Eq. 3. Moreover, we find that performance strongly improves with depth, cf. Figure 3, with a 6-layer model coming close to but still not matching a single mesa-layer.

Our probing analysis results therefore support our hypothesis that a fast descent on the autoregressive mesa-objective  $L_t(W)$  is achieved through mesa-optimization on progressively (across layers) better preconditioned data. We point to Figures A12 and A13, and Appendix A6.1.2, for an additional confirmation of this effect, showing that when taking regressed inverse probes as inputs to a linear model (instead of raw inputs  $s_t$ ), the performance of single-step learning significantly improves.

**Full-fledged Transformers.** To finish our synthetic data experiments, we relax all previous architectural simplifications and turn to training standard Transformers that use positional encodings, input and output projections, and which need to process raw tokens  $e_t = s_t$ . We hypothesize that after autoregressive training these models operate in two stages. In a first stage, they use positional information to re-create our token construction in the first softmax self-attention layer through a copying mechanism, essentially identical to first stage of the induction heads discovered by Olsson et al. (2022). This effectively corresponds to an internal *specification* of a mesa-optimization problem. Since the states are Markovian, i.e. only depend (linearly) on the immediate previous state, a simple next-token copying mechanism suffices in our toy model. The second part of our hypothesis is that subsequent layers implement a mesa-optimizer that solves the self-constructed least-squares problem. For this second part, we again use our two candidate constructions – mesa-gradient descent steps and iterative preconditioning – to guide our analyses.

Following this hypothesis, we compare three model families, namely, softmax-only Transformers, and hybrid models that have a first softmax layer followed by either linear or mesa layers. First, we verify that Transformers of all three types learn copy layers when trained on linear dynamics by



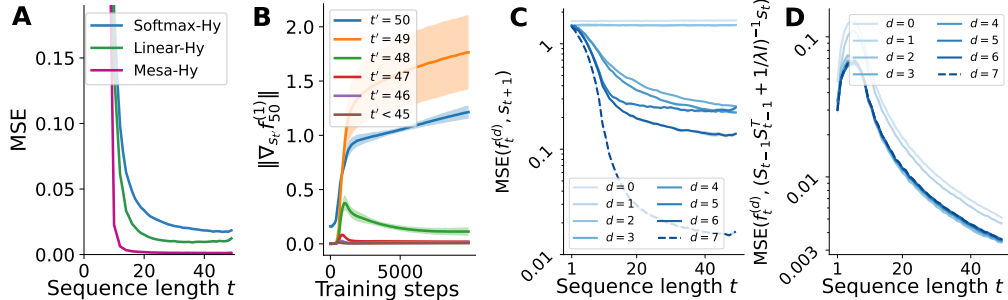


Figure 4: **Reverse engineering full-fledged trained Transformers.** We study 2-layer hybrid-mesa, 7-layer hybrid-linear, and 7-layer softmax-only Transformers. (A) After training, the hybrid-mesa Transformer slightly outperforms the deep hybrid-linear and softmax-only models in terms of autoregressive loss. In (B & C & D), we show results for a softmax-only model. The results for a linear-hybrid and an MLP-layernorm model can be found in Appendix A11, A13. (B) The first softmax layer groups together neighboring tokens. This can be seen in the high sensitivity to the current and previous tokens of the outputs of the first layer of a softmax-only Transformer (with even more clean next-token copying behavior for hybrid-linear and hybrid-mesa Transformers; see also complementary attention map visualizations in Appendix A3). (B & C) We linearly regress the activations of each layer against final targets (C) as well as  $(S_{t-1} S_{t-1}^T + 1/\lambda I)^{-1} s_t$ , the preconditioned inputs (D) predicted by our theory. Compared to our more constructed models of Figure 3, here we observe a rather harsh transition in the last layer when measuring target probing (C) while observing a gradual performance increase for early layers when probing for curvature-corrected inputs (D). These results are well aligned with our hypothesized two-stage mesa-optimizer. Averages computed over 5 different seeds; shaded area represents standard deviation.

(i) computing the sensitivity norm  $\|\nabla_{s_{t'}} f_t^{(1)}(s_{1:t}, \theta)\|$  of the output of the first layer for all  $t' \leq t$ , and by (ii) inspecting attention maps. We use  $f_t^{(d)}(s_{1:t}, \theta)$  to denote the intermediate output of the  $d$ -th layer of a Transformer, including the residual (skip connection) value. Both experiments provide evidence that after the first layer, every token mostly depends on itself and on the preceding token, as shown in Figure 4B. The corresponding attention maps as well as sensitivity analyses of all models including hybrid-linear and -mesa can be found in Appendix A3, A6.1.2.

We now turn to the post-copying behavior of the models. Although some interpretable identity structure can be observed in the weight matrix products  $W_K^T W_Q, P W_V$  of the Transformers, cf. Figures A6 and A8, we speculate that the initial embedding layer introduces too much ambiguity on how the input data is represented and processed by the subsequent attention layers, complicating reverse-engineering a clean algorithm. We therefore build on insights extracted from our previous analyses and probe hidden layer activations using the same simple linear regression analysis. Even for this more complex model, we find that again hidden activations gradually (over depth) become more predictive for both the target as well as the inverse probes. Interestingly, we observe a hard-transition-like behavior at the last layer in terms of target decoder performance, in line with our constructed two-stage mesa-optimizer, which first preconditions, and then takes an optimization step in the last layer, see Figure 4C&D and remarkably clear in Figure A11 for softmax resp. linear self-attention Transformers. We show qualitatively similar results for Transformers trained with MLPs and LayerNorm, cf. Figure A13. For experimental details, see Appendix A6.1.2.

Taken together, these findings provide evidence that realistic deep Transformers trained autoregressively on simple linear dynamics implement prediction algorithms based on mesa-optimization principles. These iterative algorithms allow a standard Transformer to harness depth to almost match the performance of a learned mesa-layer, which achieves optimality for the task considered here.

## 5.2 SIMPLE AUTOREGRESSIVE MODELS BECOME FEW-SHOT LEARNERS

In the previous section, we established a close connection between autoregressively-trained Transformers to gradient-based mesa-optimization. It is therefore natural to ask whether these models can be repurposed to learn in-context when presented with few-shot regression data. Here, we pursue this

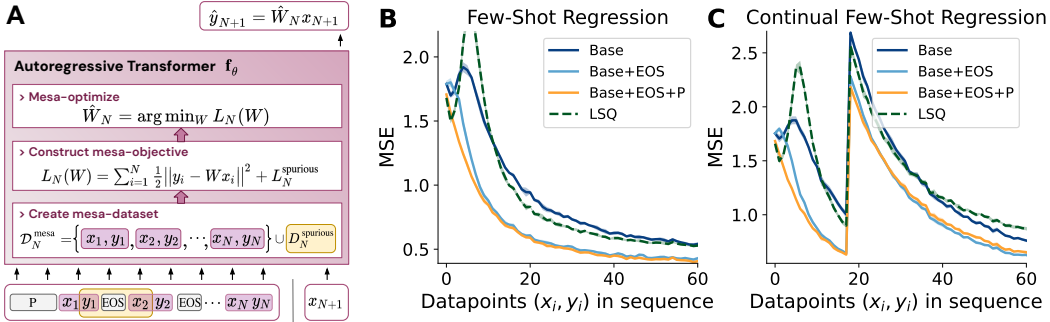


**Figure 5: Autoregressively-trained Transformers solve supervised few-shot regression problems.** (A) In-context learning by autoregressive mesa-optimization. (B) The mesa-optimization algorithm acquired by training on autoregressive linear dynamics tasks allows softmax Transformers to learn supervised tasks in-context, i.e., the mean-squared error  $\langle (f(x_i; \theta) - y_i)^2 \rangle$  decreases gradually and significantly with the number of labeled examples. When prompted with a special EOS token after each pair  $(x_i, y_i)$  or a prefix-prompt P at the beginning of an input sequence, which we fine-tune for this regression task on a held-out training set, the performance improves considerably, highlighting the usefulness of prompt-tuning already in this very simple setting. (C) Autoregressive Transformers already display some continual in-context learning capabilities, being able to learn two tasks consecutively. Here, we show the results for the full-fledged softmax-only transformer. The results for the other models can be found in Appendix A6.2. Averages computed over 5 different seeds; shaded area represents standard deviation.

question experimentally by changing the generation of the sequences *after* training, from a linear dynamical system to a linear regression task. We illustrate our findings in Figure 5A.

**Few-shot task generative model.** To generate our few-shot tasks we still sample a groundtruth  $W^*$  as a random orthogonal matrix as done during training, but now use this groundtruth model to generate a labeled training set  $\{x_i, y_i\}_{i=1}^N$ , with inputs  $x_i \sim \mathcal{N}(0, I_x)$  and targets  $y_i = W^* x_i$ . We then present this dataset to our autoregressively-trained Transformers as a sequence of tokens,  $e^{\text{few-shot}} = [x_1, y_1, \dots, x_N, y_N]$  of length  $T = 2N$ , cf. Figure 5. As the sequence unfolds, and more training data is presented, we measure in-context learning performance through the mean squared error between the Transformer output  $f_\theta(e_{2i-1}; e_{1:2i-1}^{\text{few-shot}})$  and the corresponding target  $y_i = e_{2i}$ . We emphasize that both the sequence generative model and loss function differ from the ones used during training; compare the task performance metric  $L^{\text{few-shot}} = \frac{1}{2} \sum_{i=1}^N \|e_{2i} - f_\theta(e_{2i-1}; e_{1:2i-1}^{\text{few-shot}})\|^2$  used to evaluate in-context learning performance in this section with the actual loss used to train the Transformer, Eq. 10.

**Autoregressive Transformers are capable of few-shot learning.** Although never trained on this setting, we observe that the loss of the Transformer decreases with sequence length, see Figure 5B for results obtained when taking the exact same 7-layer softmax Transformer model analyzed in Figure 4, repurposing it for in-context linear regression. The model can thus learn in-context, making use of additional in-context training data to improve its predictions. As a control, we further report the performance reached by the least-squares solution (LSQ) obtained on the dataset  $D_N^{\text{mesa}} = \{(x_i, y_i)\}_{i=1}^N \cup \{(y_i, x_{i+1})\}_{i=1}^{N-1}$ , and observe a similar decrease in loss. This dataset, where half of the associations consist of wrong input-output pairs  $D_N^{\text{spurious}} = \{(y_i, x_{i+1})\}_{i=1}^{N-1}$  as illustrated in Figure 5A, corresponds to the training set an autoregressive Transformer imbued with the mesa-optimizers uncovered in the previous section learns from. In this sense, our models achieve a few-shot learning performance that is not far from optimal. Thus, our results show that training Transformers on simple autoregressive tasks can give rise to in-context few-shot learning, complementing previous evidence for this phenomenon in large-scale models (Brown et al., 2020).

**Prompt tuning improves in-context learning performance.** To mitigate the influence of wrongly-constructed inputs  $(y_i, x_{i+1})$  in a sequence, we fine-tune a single token, which we refer to as the EOS token, to improve the in-context-learned predictions. Prompt (or prefix) tuning has been shown to lead

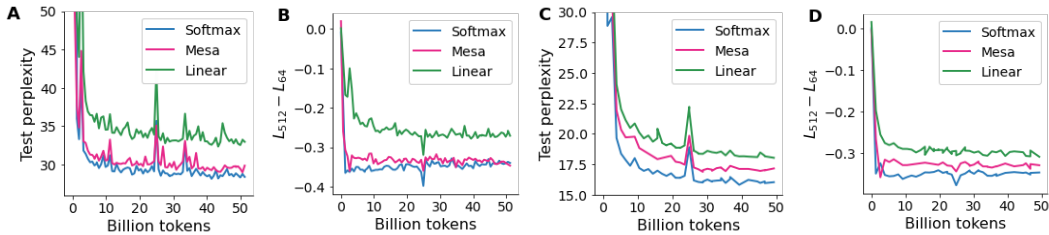


Figure 6: **Language modeling experiments on the Pile.** We observe improved perplexity and in-context learning scores across all our language modeling experiments when switching from standard linear self-attention to the mesa-layer. When comparing loss values for longer time horizons, cf. Appendix A20, we still observe a performance gap between softmax and mesa, possibly pointing towards memory issues over long sequences. As hypothesized, we confirm that in all models various copying heads can be found in the first softmax layer, see Appendix A3 for visualizations of the attention heads. **(A&B)** 2-layer Transformers without MLPs and first layers softmax self-attention and second layer either softmax, mesa or linear. **(C&D)** 4-layer Transformers with MLPs and first layers softmax self-attention and rest of the layers either all softmax, mesa or linear.

to significant performance improvements when applied to large language models (Li & Liang, 2021; Lester et al., 2021); here we investigate the effectiveness of this technique on our mechanistically-understood models. When presenting data sequentially as  $[x_1, y_1, \text{EOS}, x_2, y_2, \dots, \text{EOS}, x_N, y_N]$  we observe a considerable performance improvement after prompt-tuning, see Figure 5B. Furthermore, to ‘guide’ the model for few-shot tasks, we learn a single prefix-prompt  $\mathcal{P}$  which we append at the beginning of a sequence with EOS tokens. This appears to further improve the few-shot performance for early data-pairs. Additional experimental details can be found in Appendix A6.2.

**Continual in-context learning.** Lastly, we demonstrate the capability of our trained Transformers to learn multiple tasks in a row. We study the minimal setup where the model has to learn two tasks, generated from two distinct groundtruth linear models with parameters  $W^{*,1}, W^{*,2}$  sampled as described above, resulting in a sequence of data of the form  $[x_1^1, y_1^1, \dots, x_N^1, y_N^1, x_1^2, y_1^2, \dots, x_N^2, y_N^2]$ . We plot the performance when using EOS tokens (constructed as before) and prefix prompts  $\mathcal{P}$ , as well. In Figure 5C we see that the trained Transformer has the capability to overwrite the first and learn a second task in-context, even though it was never explicitly trained to solve such sequential learning problems.

**A toy model for in-context learning.** We conclude that Transformers trained to predict the next element in a sequence can be naturally repurposed as in-context learners due to the similarity of the algorithms implemented within their forward pass. This allows studying in a controlled setting interesting properties of in-context learning, such as the advantages of prompt tuning and the ability to learn continually. Our toy models could serve as a test bed for future work investigating the shortcomings and various particularities of in-context learning observed in LLMs (e.g., Chan et al., 2022a; Min et al., 2022; Kossen et al., 2023).

### 5.3 LANGUAGE MODELS EQUIPPED WITH LEAST-SQUARES SOLVERS

We now move beyond synthetic tasks and provide results on autoregressive language modeling, a problem domain Transformers have revolutionized in recent years. Because reverse-engineering the ensuing models to the degree of our previous analyses is difficult, we base our claims on performance comparisons between standard Transformers, and new variants based on the mesa-layer. Our hypothesis is that the mesa-layer will improve the in-context learning and working memory capabilities of a Transformer, in particular of the linear kind. We further hypothesize that this in turn translates to language modeling improvements, based on the high correlation between in-context learning and actual autoregressive loss reported by Kaplan et al. (2020). We therefore quantify performance along two axes: the next-token prediction loss, the actual objective of base-optimization; and the ability to learn in-context, measured as the difference in loss calculated over two timepoints within a sequence, as defined by Kaplan et al. (2020) and Olsson et al. (2022).

We train Transformers with various architectural configurations on the Pile (Gao et al., 2020), a large compilation of various English text datasets including parts of Wikipedia, arXiv, and code. We always model the first layer using softmax self-attention in all experiments. This decision is based on insights from our previous experiments, where base-optimization consistently attributed a mesa-objective creation role to this layer. We then compare pure softmax-only Transformers to two types of hybrid models, where the subsequent layers are either linear or mesa. We vary the depth of our models, from 2-layer attention-only to deeper 4-attention-layer models endowed with tokenwise MLPs which are present by default in standard Transformers. By transforming the data nonlinearly, MLP layers allow solving nonlinear regression problems by mesa-gradient descent. Following this reasoning, we further adopt in our hybrid-linear and hybrid-mesa Transformers the deterministic parameter-free projection (DPFP, size denoted by  $\nu$ ) due to Schlag et al. (2021), a non-learned and simple to compute nonlinear transformation of keys and queries. We found that this significantly improved the performance of non-softmax attention layers. Finally, to represent discrete input symbols as real-valued vectors, we learn a vocabulary of real-valued vectors using the standard GPT-2 tokenizer. All architectural and training details can be found in Appendix A6.3. We note that all models have an (almost) identical number of parameters.

In line with our synthetic experiments, we observe stable learning across all model types of copying layers, indicated by the constant attention to tokens in direct or close proximity, as shown in Figure A1. We therefore reproduce the findings of Olsson et al. (2022), extending them to models that include other forms of attention. This phenomenon is predicted by the mesa-optimization theory presented here, where copy layers serve the purpose of constructing internal mesa-objective functions. We note that, in contrast to our previous synthetic linear prediction tasks, the Pile is no longer Markovian of order 1. This is reflected in the more complicated attention maps, indicating more involved copying behavior. Additionally, we run an ablation where we compare to a single-layer control model whose first softmax layer is removed and replaced by a hardcoded one-step key-shift operator, cf. Appendix A6.3. Interestingly, such an operator can be found in previous work (Olsson et al., 2022; Fu et al., 2023). Again, we verify the findings of Olsson et al. (2022) and observe strong in-context learning scores, within a single layer, with the mesa-layer performing on-par with softmax, see Figure 7. As in Schlag et al. (2021), DPFP features substantially improve performance; we fix  $\nu = 3$  for the linear as well as the mesa layer for all other language modeling experiments.

We find that the hybrid-mesa Transformers dominate their hybrid-linear counterparts in terms of performance, across all configurations, essentially matching (for 2-layer models) or coming closer (for 4-layer models with MLPs) to pure-softmax Transformers, cf. Figure 6. We leave for future work studying the mesa-layer equipped with forgetting factors, see Appendix A2.1, which could further improve upon our results here. This is reflected both in terms of perplexity and in-context learning scores. Strictly speaking, these results are not sufficient to make claims on whether mesa-optimization is occurring within standard Transformers. However, the high performance achieved by the hybrid-mesa models, which operate on mesa-optimization principles by design, suggests that mesa-optimization might be happening within conventional Transformers. More reverse-engineering work is needed to add weight to this conjecture.

## 6 DISCUSSION

We presented evidence that Transformer models are capable of developing gradient-based inference algorithms when trained on sequence prediction tasks under a standard autoregressive objective. We therefore confirmed that recent results obtained under a multi-task, meta-learning setup translate to the conventional self-supervised LLM training setup. Moreover, we have seen that the resulting

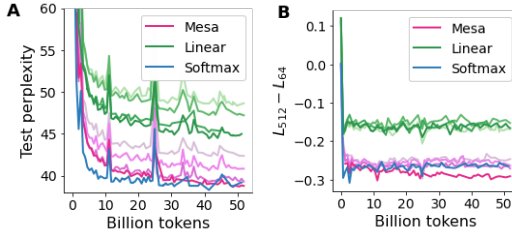


Figure 7: **Single-layer Transformers with key-shifts, the Pile.** We observe improved (A) perplexity and (B) in-context learning scores when comparing one linear to one mesa layer with different DPFP sizes  $\nu \in \{0, 1, 2, 3\}$ , corresponding inversely to color fade. Mesa layers consistently outperform linear layers, catching up with softmax.

autoregressive inference algorithms can be repurposed without retraining to solve supervised in-context learning tasks, thus explaining the aforementioned results within a single, unified framework.

It should be noted that our reverse-engineering findings are for now restricted to simple linear prediction tasks. More work is needed to understand how and if our findings translate to the nonlinear setting, and more generally to determine the conditions that lead some base optimization process to pick solutions corresponding to gradient-based in-context learning algorithms. It seems unlikely that the internal construction and gradient-based solution of least-squares problems is a universal mechanistic explanation of trained Transformers. An interesting future work direction is to attempt to reverse-engineer and describe through mesa-optimization models trained on problems of a radically different kind than those considered here, such as algorithmic reasoning (Liu et al., 2023).

The idea that a Transformer generates its predictions by solving one or more internal optimization problems has ties to many different lines of thinking in machine learning. One closely related line of work explores the concept of a declarative node: a differentiable layer whose output is defined implicitly as the solution of an optimization problem (Amos & Kolter, 2017; Gould et al., 2021; Zucchet & Sacramento, 2022). The mesa-layer is an example of such a node. Summarizing the operation of an entire chain of layers with thousands of parameters by a single declarative node is not only potentially more efficient, but also more interpretable. We thus join a line of interesting recent work exploring the advantages of including declarative nodes within attention-based models (Martins et al., 2020; Garnelo & Czarnecki, 2023).

Our reverse-engineering analyses brought a surprising revelation: gradient-based base-optimization of an autoregressive loss *discovered* such a declarative node, at least when the underlying sequence was generated by a linear dynamics. This discovery or selection of an optimization algorithm through learning has been termed mesa-optimization (Hubinger et al., 2019), a notion that we have adopted throughout this paper. While we do not wish to comment here on the possible risks associated with mesa-optimization, we point out that our results may be of interest to the artificial intelligence safety community, by providing a simple mesa-optimization toy model.

The mesa-layer can also be seen as a locally-optimal fast weight programmer from the perspective of Schmidhuber (1992). In his seminal work, Schmidhuber (1992) proposed to dynamically reprogram the weights of a feedforward neural network using a Hebbian rule. As pointed out by Schlag et al. (2021) and as can be seen from Eq. 2, this is precisely what a linear self-attention layer does: it generates predictions using an effective weight matrix that is learned during a forward pass by taking outer products of values and keys, a Hebbian associative rule (Hebb, 1949). In this work, we instead frame fast weight learning as an optimization problem, that is efficiently and optimally solved at every moment in time by the mesa-layer. This form of optimal fast learning is strictly superior to Hebb’s rule, both in terms of generalization and memory capacity (Hertz et al., 1991). The mesa-layer is therefore also closely related to the Delta-Net of Schlag et al. (2021), which uses the delta rule (Widrow & Hoff, 1960) for fast weight learning. Unlike the mesa-layer which is optimal at every time step, this rule requires multiple steps to converge, but it is cheaper to implement.

When using mesa-layers in an autoregressive Transformer, the base-optimization process becomes explicitly a meta-learning algorithm (Thrun & Pratt, 1998). This algorithm should however be distinguished from the end-to-end supervised meta-learning approaches that are currently highly popular in machine learning (e.g., Ravi & Larochelle, 2017; Finn et al., 2017; Hochreiter et al., 2001). In our models, everything is ultimately driven by the pressure to predict the future, the signal that drives the slow autoregressive base-optimization process. This process ultimately dictates the objectives each layer must optimize. Moreover and also unusually for meta-learning, each mesa-layer is a greedy supervised local learner, which does not use backpropagation or any other kind of global error information. Instead, each mesa-layer has its own local objective functions specified through the corresponding key and value matrices.

Seen from this angle, our work has an unexpected connection to research on local learning rules, a question of great interest in theoretical neuroscience (Lillicrap et al., 2020). Decomposing a global supervised learning problem into a sequence of local quadratic optimization problems, as we do here, is at the heart of the target propagation (Lee et al., 2015), predictive coding (Whittington & Bogacz, 2017) and control-based (Meulemans et al., 2022) theories of learning in the brain, and previous studies have proposed greedy layerwise learning algorithms that do not require global error information (Hinton et al., 2006; Nøkland & Eidnes, 2019; Belilovsky et al., 2019; Löwe

et al., 2019; Hinton, 2022). Our study introduces greedy local learning algorithms, which only use bottom-up information, to the fast timescale of inference. It is interesting that our models achieve strong performance in natural tasks without any top-down feedback at fast timescales, at odds with canonical predictive coding theories (Mumford, 1992; Rao & Ballard, 1999).

We finish by sharing our excitement about future research directions that aim at analyzing simple autoregressively-trained sequence models like Transformers and in particular in-context learning within by reverse engineering. We hope our work motivates further studies trying to describe the emergence of single, multiple or mixture of expert models mesa-optimized in simple trained Transformers (Bai et al., 2023) which we hypothesize could illicit inference reminiscent to world models (Ha & Schmidhuber, 2018; Werbos, 1987). Furthermore, the insights we gained in our controlled setting could motivate studying limitations and particularities of in-context learning (Min et al., 2022; Kossen et al., 2023) and its powerful variants such as chain-of-thought prompting (Wei et al., 2022; Li et al., 2023b; Giannou et al., 2023) as well as the fascinating interplay between in-weights and in-context learning (Chan et al., 2022b).

#### ACKNOWLEDGMENTS

João Sacramento and Johannes von Oswald deeply thank Angelika Steger and Jyrki Alakuijala for their support and guidance. The authors also thank Marc Kaufmann and Yassir Akram for many valuable insights throughout the project and especially thank Andrey Zhmoginov for many fruitful discussions. Furthermore, we are grateful to Luke Sernau and Alexander Meulemans providing valuable comments on the manuscript. João Sacramento and Nicolas Zucchet were supported by an Ambizione grant (PZ00P3\_186027) from the Swiss National Science Foundation and an ETH Research Grant (ETH-23 21-1).

#### REFERENCES

- Kwangjun Ahn, Xiang Cheng, Hadi Daneshmand, and Suvrit Sra. Transformers learn to implement preconditioned gradient descent for in-context learning. *arXiv preprint arXiv:2306.00297*, 2023.
- Ekin Akyürek, Dale Schuurmans, Jacob Andreas, Tengyu Ma, and Denny Zhou. What learning algorithm is in-context learning? Investigations with linear models. In *International Conference of Learning Representations*, 2023.
- Guillaume Alain and Yoshua Bengio. Understanding intermediate layers using linear classifier probes. In *International Conference of Learning Representations*, 2017.
- Brandon Amos and J. Zico Kolter. OptNet: Differentiable optimization as a layer in neural networks. In *International Conference on Machine Learning*, 2017.
- Jimmy Lei Ba, Jamie Ryan Kiros, and Geoffrey E. Hinton. Layer normalization. *arXiv preprint 1607.06450*, 2016.
- Igor Babuschkin, Kate Baumli, Alison Bell, Surya Bhupatiraju, Jake Bruce, Peter Buchlovsky, David Budden, Trevor Cai, Aidan Clark, Ivo Danihelka, Antoine Dedieu, Claudio Fantacci, Jonathan Godwin, Chris Jones, Ross Hemsley, Tom Hennigan, Matteo Hessel, Shaobo Hou, Steven Kapturowski, Thomas Keck, Iurii Kemaev, Michael King, Markus Kunesch, Lena Martens, Hamza Merzic, Vladimir Mikulik, Tamara Norman, George Papamakarios, John Quan, Roman Ring, Francisco Ruiz, Alvaro Sanchez, Laurent Sartran, Rosalia Schneider, Eren Sezener, Stephen Spencer, Srivatsan Srinivasan, Miloš Stanojević, Wojciech Stokowiec, Luyu Wang, Guangyao Zhou, and Fabio Viola. The DeepMind JAX Ecosystem, 2020.
- Dzmitry Bahdanau, Kyunghyun Cho, and Yoshua Bengio. Neural machine translation by jointly learning to align and translate. In *International Conference of Learning Representations*, 2015.
- Yu Bai, Fan Chen, Huan Wang, Caiming Xiong, and Song Mei. Transformers as statisticians: provable in-context learning with in-context algorithm selection. *arXiv preprint arXiv:2306.04637*, 2023.
- Eugene Belilovsky, Michael Eickenberg, and Edouard Oyallon. Greedy layerwise learning can scale to ImageNet. In *International Conference on Machine Learning*, 2019.

- James Bradbury, Roy Frostig, Peter Hawkins, Matthew James Johnson, Chris Leary, Dougal Maclaurin, George Necula, Adam Paszke, Jake VanderPlas, Skye Wanderman-Milne, and Qiao Zhang. JAX: composable transformations of Python+NumPy programs, 2018.
- Tom B. Brown, Benjamin Mann, Nick Ryder, Melanie Subbiah, Jared Kaplan, Prafulla Dhariwal, Arvind Neelakantan, Pranav Shyam, Girish Sastry, Amanda Askell, Sandhini Agarwal, Ariel Herbert-Voss, Gretchen Krueger, Tom Henighan, Rewon Child, Aditya Ramesh, Daniel M. Ziegler, Jeffrey Wu, Clemens Winter, Christopher Hesse, Mark Chen, Eric Sigler, Mateusz Litwin, Scott Gray, Benjamin Chess, Jack Clark, Christopher Berner, Sam McCandlish, Alec Radford, Ilya Sutskever, and Dario Amodei. Language models are few-shot learners. In *Advances in Neural Information Processing Systems*, volume 33, 2020.
- Stephanie C. Y. Chan, Ishita Dasgupta, Junkyung Kim, Dharshan Kumaran, Andrew K. Lampinen, and Felix Hill. Transformers generalize differently from information stored in context vs in weights. *arXiv preprint arXiv:2210.05675*, 2022a.
- Stephanie C. Y. Chan, Adam Santoro, Andrew K. Lampinen, Jane X. Wang, Aaditya Singh, Pierre H. Richemond, Jay McClelland, and Felix Hill. Data distributional properties drive emergent in-context learning in transformers. *Advances in Neural Information Processing Systems*, 35, 2022b.
- Krzysztof Choromanski, Valerii Likhoshesterov, David Dohan, Xingyou Song, Andreea Gane, Tamas Sarlos, Peter Hawkins, Jared Davis, Afroz Mohiuddin, Lukasz Kaiser, David Belanger, Lucy Colwell, and Adrian Weller. Rethinking attention with performers. In *International Conference of Learning Representations*, 2021.
- Jacob Devlin, Ming-Wei Chang, Kenton Lee, and Kristina Toutanova. BERT: Pre-training of Deep Bidirectional Transformers for Language Understanding. In *Proceedings of NAACL-HLT*, 2019.
- Nan Ding, Tomer Levinboim, Jialin Wu, Sebastian Goodman, and Radu Soricut. CausalLM is not optimal for in-context learning. *arXiv preprint arXiv:2308.06912*, 2023.
- Chelsea Finn, Pieter Abbeel, and Sergey Levine. Model-agnostic meta-learning for fast adaptation of deep networks. In *International Conference on Machine Learning*, 2017.
- Quentin Fournier, Gaétan Marceau Caron, and Daniel Aloise. A practical survey on faster and lighter transformers. *ACM Computing Surveys*, 55(14s), 2023.
- Daniel Y. Fu, Tri Dao, Khaled K. Saab, Armin W. Thomas, Atri Rudra, and Christopher Ré. Hungry hungry hippos: towards language modeling with state space models. In *International Conference of Learning Representations*, 2023.
- Leo Gao, Stella Biderman, Sid Black, Laurence Golding, Travis Hoppe, Charles Foster, Jason Phang, Horace He, Anish Thite, Noa Nabeshima, Shawn Presser, and Connor Leahy. The pile: an 800GB dataset of diverse text for language modeling. *arXiv preprint arXiv:2101.00027*, 2020.
- Shivam Garg, Dimitris Tsipras, Percy S. Liang, and Gregory Valiant. What can transformers learn in-context? A case study of simple function classes. In *Advances in Neural Information Processing Systems*, volume 35, 2022.
- Marta Garnelo and Wojciech Marian Czarnecki. Exploring the space of key-value-query models with intention. *arXiv preprint arXiv:2305.10203*, 2023.
- Carl Friedrich Gauss. *Theoria combinationis observationum: erroribus minimis obnoxiae*. Societas Regia Scientiarum Gottingensis, 1821.
- Angeliki Giannou, Shashank Rajput, Jy-yong Sohn, Kangwook Lee, Jason D. Lee, and Dimitris Papailiopoulos. Looped transformers as programmable computers. In *International Conference on Machine Learning*, 2023.
- Stephen Gould, Richard Hartley, and Dylan John Campbell. Deep declarative networks. *IEEE Transactions on Pattern Analysis and Machine Intelligence*, 2021.
- David Ha and Jürgen Schmidhuber. World models. *arXiv preprint arXiv:1803.10122*, 2018.

- Richard H. R. Hahnloser, Rahul Sarpeshkar, Misha A. Mahowald, Rodney J. Douglas, and H. Sebastian Seung. Digital selection and analogue amplification coexist in a cortex-inspired silicon circuit. *Nature*, 405(6789):947–951, 2000.
- Charles R. Harris, K. Jarrod Millman, Stéfan J. van der Walt, Ralf Gommers, Pauli Virtanen, David Cournapeau, Eric Wieser, Julian Taylor, Sebastian Berg, Nathaniel J. Smith, Robert Kern, Matti Picus, Stephan Hoyer, Marten H. van Kerkwijk, Matthew Brett, Allan Haldane, Jaime Fernández del Río, Mark Wiebe, Pearu Peterson, Pierre Gérard-Marchant, Kevin Sheppard, Tyler Reddy, Warren Weckesser, Hameer Abbasi, Christoph Gohlke, and Travis E. Oliphant. Array programming with NumPy. *Nature*, 585(7825):357–362, 2020.
- Donald O. Hebb. *The Organization of Behavior: A Neuropsychological Theory*. Wiley, New York, 1949.
- Jonathan Heek, Anselm Levskaya, Avital Oliver, Marvin Ritter, Bertrand Rondepierre, Andreas Steiner, and Marc van Zee. Flax: A neural network library and ecosystem for JAX, 2023.
- Tom Hennigan, Trevor Cai, Tamara Norman, Lena Martens, and Igor Babuschkin. Haiku: Sonnet for JAX, 2020.
- John Hertz, Richard G. Palmer, and Anders S. Krogh. *Introduction to the Theory of Neural Computation*. Perseus Publishing, 1st edition, 1991.
- Geoffrey Hinton. The forward-forward algorithm: Some preliminary investigations. *arXiv preprint arXiv:2212.13345*, 2022.
- Geoffrey Hinton, Simon Osindero, and Yee Whye Teh. A Fast Learning Algorithm for Deep Belief Nets. *Neural Computation*, 18:1527–1554, 2006.
- Sepp Hochreiter, A. Steven Younger, and Peter R. Conwell. Learning to learn using gradient descent. In *Artificial Neural Networks — ICANN 2001*, 2001.
- Evan Hubinger, Chris van Merwijk, Vladimir Mikulik, Joar Skalse, and Scott Garrabrant. Risks from learned optimization in advanced machine learning systems. *arXiv preprint 1906.01820*, 2019.
- J. D. Hunter. Matplotlib: A 2D graphics environment. *Computing in Science & Engineering*, 9(3): 90–95, 2007.
- Richard M. Johnstone, C. Richard Johnson, Robert R. Bitmead, and Brian D. O. Anderson. Exponential convergence of recursive least squares with exponential forgetting factor. *Systems & Control Letters*, 2(2):77–82, 1982.
- Jared Kaplan, Sam McCandlish, Tom Henighan, Tom B Brown, Benjamin Chess, Rewon Child, Scott Gray, Alec Radford, Jeffrey Wu, and Dario Amodei. Scaling laws for neural language models. *arXiv preprint arXiv:2001.08361*, 2020.
- Angelos Katharopoulos, Apoorv Vyas, Nikolaos Pappas, and François Fleuret. Transformers are RNNs: fast autoregressive transformers with linear attention. In *International Conference on Machine Learning*, 2020.
- Diederik P. Kingma and Jimmy Ba. Adam: a method for stochastic optimization. In *International Conference on Learning Representations*, 2015.
- Louis Kirsch, James Harrison, Jascha Sohl-Dickstein, and Luke Metz. General-purpose in-context learning by meta-learning transformers. In *Sixth Workshop on Meta-Learning at the Conference on Neural Information Processing Systems*, 2022.
- Jannik Kossen, Tom Rainforth, and Yarin Gal. In-context learning in large language models learns label relationships but is not conventional learning. *arXiv preprint arXiv:2307.12375*, 2023.
- Dong-Hyun Lee, Saizheng Zhang, Asja Fischer, and Yoshua Bengio. Difference target propagation. In *Joint European Conference on Machine Learning and Knowledge Discovery in Databases*, 2015.



- Brian Lester, Rami Al-Rfou, and Noah Constant. The power of scale for parameter-efficient prompt tuning. In *Proceedings of the 2021 Conference on Empirical Methods in Natural Language Processing*, 2021.
- Xiang Lisa Li and Percy Liang. Prefix-tuning: optimizing continuous prompts for generation. In *Proceedings of the 59th Annual Meeting of the Association for Computational Linguistics*, 2021.
- Yingcong Li, Muhammed Emrullah Ildiz, Dimitris Papailiopoulos, and Samet Oymak. Transformers as algorithms: Generalization and stability in in-context learning. In *International Conference on Machine Learning*, 2023a.
- Yingcong Li, Kartik Sreenivasan, Angeliki Giannou, Dimitris Papailiopoulos, and Samet Oymak. Dissecting chain-of-thought: a study on compositional in-context learning of MLPs. *arXiv preprint arXiv:2305.18869*, 2023b.
- Timothy P. Lillicrap, Adam Santoro, Luke Marris, Colin J. Akerman, and Geoffrey Hinton. Back-propagation and the brain. *Nature Reviews Neuroscience*, 21(6):335–346, 2020.
- Bingbin Liu, Jordan T. Ash, Surbhi Goel, Akshay Krishnamurthy, and Cyril Zhang. Transformers learn shortcuts to automata. *arXiv preprint arXiv:2210.10749*, 2023.
- Sindy Löwe, Peter O’Connor, and Bastiaan Veeling. Putting an end to end-to-end: Gradient-isolated learning of representations. In *Advances in Neural Information Processing Systems*, volume 32, 2019.
- Arvind Mahankali, Tatsunori B. Hashimoto, and Tengyu Ma. One step of gradient descent is provably the optimal in-context learner with one layer of linear self-attention. *arXiv preprint arXiv:2307.03576*, 2023.
- André Martins, António Farinhas, Marcos Treviso, Vlad Niculae, Pedro Aguiar, and Mario Figueiredo. Sparse and continuous attention mechanisms. In *Advances in Neural Information Processing Systems*, volume 33, 2020.
- Alexander Meulemans, Nicolas Zucchet, Seijin Kobayashi, Johannes von Oswald, and João Sacramento. The least-control principle for local learning at equilibrium. In *Advances in Neural Information Processing Systems*, volume 35, 2022.
- Sewon Min, Xinxu Lyu, Ari Holtzman, Mikel Artetxe, Mike Lewis, Hannaneh Hajishirzi, and Luke Zettlemoyer. Rethinking the role of demonstrations: what makes in-context learning work? In *Proceedings of the 2022 Conference on Empirical Methods in Natural Language Processing*, 2022.
- David Mumford. On the computational architecture of the neocortex. *Biological Cybernetics*, 66(3): 241–251, 1992.
- Arild Nøklund and Lars Hiller Eidnes. Training neural networks with local error signals. In *International Conference on Machine Learning*, 2019.
- Catherine Olsson, Nelson Elhage, Neel Nanda, Nicholas Joseph, Nova DasSarma, Tom Henighan, Ben Mann, Amanda Askell, Yuntao Bai, Anna Chen, Tom Conerly, Dawn Drain, Deep Ganguli, Zac Hatfield-Dodds, Danny Hernandez, Scott Johnston, Andy Jones, Jackson Kernion, Liane Lovitt, Kamal Ndousse, Dario Amodei, Tom Brown, Jack Clark, Jared Kaplan, Sam McCandlish, and Chris Olah. In-context learning and induction heads. *Transformer Circuits Thread*, 2022.
- Rajesh P. N. Rao and Dana H. Ballard. Predictive coding in the visual cortex: a functional interpretation of some extra-classical receptive-field effects. *Nature Neuroscience*, 2(1):79–87, 1999.
- Allan Raventós, Mansheej Paul, Feng Chen, and Surya Ganguli. Pretraining task diversity and the emergence of non-Bayesian in-context learning for regression. *arXiv preprint arXiv:2306.15063*, 2023.
- Sachin Ravi and Hugo Larochelle. Optimization as a model for few-shot learning. In *International Conference on Learning Representations*, 2017.

- Imanol Schlag, Kazuki Irie, and Jürgen Schmidhuber. Linear transformers are secretly fast weight programmers. In *International Conference on Machine Learning*, 2021.
- Jürgen Schmidhuber. Learning to control fast-weight memories: an alternative to dynamic recurrent networks. *Neural Computation*, 4(1):131–139, 1992.
- Jack Sherman and Winifred J. Morrison. Adjustment of an inverse matrix corresponding to a change in one element of a given matrix. *The Annals of Mathematical Statistics*, 21(1):124–127, 1950.
- Sebastian Thrun and Lorien Pratt. *Learning to learn*. Springer US, 1998.
- Marcos Treviso, Ji-Ung Lee, Tianchu Ji, Betty van Aken, Qingqing Cao, Manuel R. Ciosici, Michael Hassid, Kenneth Heafield, Sara Hooker, Colin Raffel, Pedro H. Martins, André F. T. Martins, Jessica Zosa Forde, Peter Milder, Edwin Simpson, Noam Slonim, Jesse Dodge, Emma Strubell, Niranjana Balasubramanian, Leon Derczynski, Iryna Gurevych, and Roy Schwartz. Efficient methods for natural language processing: a survey. *Transactions of the Association for Computational Linguistics*, 11, 2023.
- Ashish Vaswani, Noam Shazeer, Niki Parmar, Jakob Uszkoreit, Llion Jones, Aidan N. Gomez, Lukasz Kaiser, and Illia Polosukhin. Attention is all you need. In *Advances in Neural Information Processing Systems*, volume 30, 2017.
- Johannes von Oswald, Eyvind Niklasson, Ettore Randazzo, João Sacramento, Alexander Mordvintsev, Andrey Zhmoginov, and Max Vladymyrov. Transformers learn in-context by gradient descent. In *International Conference on Machine Learning*, 2023.
- Sinong Wang, Belinda Z. Li, Madian Khabsa, Han Fang, and Hao Ma. Linformer: self-attention with linear complexity. *arXiv preprint arXiv:2006.04768*, 2020.
- Jason Wei, Xuezhi Wang, Dale Schuurmans, Maarten Bosma, Brian Ichter, Fei Xia, Ed Chi, Quoc Le, and Denny Zhou. Chain-of-thought prompting elicits reasoning in large language models. In *Advances in Neural Information Processing Systems*, volume 35, 2022.
- Paul J. Werbos. Learning how the world works: Specifications for predictive networks in robots and brains. In *Proceedings of IEEE International Conference on Systems, Man and Cybernetics, NY*, 1987.
- James C. R. Whittington and Rafal Bogacz. An approximation of the error backpropagation algorithm in a predictive coding network with local Hebbian synaptic plasticity. *Neural Computation*, 29(5): 1229–1262, 2017.
- Bernard Widrow and Marcian E. Hoff. Adaptive switching circuits. In *IRE WESCON convention record*, volume 4, 1960.
- Sang Michael Xie, Aditi Raghunathan, Percy Liang, and Tengyu Ma. An explanation of in-context learning as implicit Bayesian inference. In *International Conference of Learning Representations*, 2022.
- Ruiqi Zhang, Spencer Frei, and Peter L. Bartlett. Trained transformers learn linear models in-context. *arXiv preprint arXiv:2306.09927*, 2023.
- Nicolas Zucchet and João Sacramento. Beyond backpropagation: bilevel optimization through implicit differentiation and equilibrium propagation. *Neural Computation*, 34(12), 2022.

## Appendix

### Table of Contents

<b>A1 Mesa layer with forgetting factors</b>	<b>19</b>
A1.1 Computing the inverse term within $\hat{W}_t^{\text{mesa}}$	20
A1.2 Computing $\Delta e_t^{\text{mesa}}$	20
<b>A2 Mesa layer backward computation</b>	<b>20</b>
A2.1 Mesa layer computation backward pass via Sherman-Morrison	20
A2.2 Alternative derivation through the implicit function theorem	22
A2.3 Parallel backward pass through Neumann series approximation	23
<b>A3 Visualization of weights and attention maps of trained Transformers</b>	<b>25</b>
<b>A4 Mechanistic interpretability of Transformers trained on linear dynamics</b>	<b>31</b>
A4.1 Single-layer mesa-gradient descent	31
A4.2 Multi-layer accelerated mesa-gradient descent	33
<b>A5 Analysing contracting linear dynamics</b>	<b>36</b>
<b>A6 Experimental details</b>	<b>36</b>
A6.1 Training Transformers on linear dynamical systems	36
A6.2 Testing trained Transformers on few-shot in-context learning	40
A6.3 Language modeling experiments	45
<b>A7 Software</b>	<b>45</b>

#### A1 MESA LAYER WITH FORGETTING FACTORS

Here, we revisit the mesa-layer forward pass introduced in Section 4, with an added forget factor  $\Gamma_{h,t} = (\gamma_{h,t'})_{t'=1}^t$ , where  $\gamma_{h,t'} \in (0, 1]$ .

Although we leave an empirical investigation of the forget gate for future work, we hypothesize that a token-dependent forget gate can benefit the performance of the layer by allowing selective memory retention and forgetting. Nevertheless, we stress potential initialization and numerical issues as well as training instabilities when computing the necessary products of factors across time.

Given again a set of tokens  $E_t$ , the generalized mesa-layer changes the tokens as follows:

$$\Delta e_t^{\text{mesa}} = \sum_{h=1}^H P_h \hat{W}_{h,t}^{\text{mesa}} q_{h,t}, \quad (\text{A1})$$

$$\text{with } \hat{W}_{h,t}^{\text{mesa}} = \arg \min_W \left\{ \frac{1}{2} \sum_{t'=1}^t \left( \prod_{t''=t'+1}^t \gamma_{h,t''} \right) \|W k_{h,t'} - v_{h,t'}\|^2 + \frac{\prod_{t''=1}^t \gamma_{h,t''}}{2\lambda_h} \|W\|_{\text{F}}^2 \right\}. \quad (\text{A2})$$

This is known as the recursive least squares problem with forgetting and is widely used in the online learning literature (Johnstone et al., 1982). For notational simplicity we drop the subscript in  $h$  and ignore the sum over the heads in the following derivation. It can be shown that the analytical solution of the optimization problem is

$$\hat{W}_t^{\text{mesa}} = \left( \sum_{t'=1}^t \left( \prod_{t''=t'+1}^t \gamma_{t''} \right) v_{t'} k_{t'}^\top \right) \left( \sum_{t'=1}^t \left( \prod_{t''=t'+1}^t \gamma_{t''} \right) k_{t'} k_{t'}^\top + \frac{\prod_{t''=1}^t \gamma_{t''}}{\lambda} I \right)^{-1} \quad (\text{A3})$$

We will now see how  $\Delta e_t^{\text{mesa}}$  can be efficiently computed in a forward pass.

### A1.1 COMPUTING THE INVERSE TERM WITHIN $\hat{W}_t^{\text{mesa}}$

Computing the full-fledged inverse at every timestep is computationally too expensive. As in Section 4, we resort to using the Sherman-Morrison formula to efficiently compute the inverse term for all timestep sequentially in time. We redefine

$$R_t = \left( \sum_{t'=1}^t \left( \prod_{t''=t'+1}^t \gamma_{t''} \right) k_{t'} k_{t'}^\top + \frac{\prod_{t''=1}^t \gamma_{t''}}{\lambda} I \right)^{-1}. \quad (\text{A4})$$

It satisfies the recursive formula

$$R_{t+1} = (\gamma_t R_t^{-1} + k_{t+1} k_{t+1}^\top)^{-1} \quad (\text{A5})$$

with  $R_0 = \lambda I$ , and the Sherman-Morrison formula thus gives

$$R_{t+1} = \gamma_{t+1}^{-1} (R_t^{-1} + \gamma_{t+1}^{-1} k_{t+1} k_{t+1}^\top)^{-1} \quad (\text{A6})$$

$$= \gamma_{t+1}^{-1} \left( R_t - \frac{\gamma_{t+1}^{-1} R_t k_{t+1} k_{t+1}^\top R_t}{1 + \gamma_{t+1}^{-1} k_{t+1}^\top R_t k_{t+1}} \right) \quad (\text{A7})$$

$$= \gamma_{t+1}^{-1} \left( R_t - \frac{R_t k_{t+1} k_{t+1}^\top R_t}{\gamma_{t+1} + k_{t+1}^\top R_t k_{t+1}} \right). \quad (\text{A8})$$

Note that we recover Eq. 8 by setting all  $\gamma_t$  to 1.

### A1.2 COMPUTING $\Delta e_t^{\text{mesa}}$

Given  $R_{h,t}$  for all heads, we can rewrite the token update as

$$\Delta e_t^{\text{mesa}} = \sum_{h=1}^H P_h \left( \sum_{t'=1}^t \left( \prod_{t''=t'+1}^t \gamma_{h,t''} \right) v_{h,t'} k_{h,t'}^\top \right) R_{h,t} q_{h,t} \quad (\text{A9})$$

$$= \sum_{h=1}^H P_h V_h \left( \left( \mathbb{1}_{t' \leq t} \prod_{t''=t'+1}^t \gamma_{h,t''} \right)_{t'=1}^\top \odot K_h^\top \tilde{q}_{h,t} \right) \quad (\text{A10})$$

$$= \sum_{h=1}^H P_h V_h (M_{:,t} \odot K_h^\top \tilde{q}_{h,t}) \quad (\text{A11})$$

where  $\tilde{q}_{h,t} = R_{h,t} q_{h,t}$  and  $M_{t',t} := \mathbb{1}_{t' \leq t} \prod_{t''=t'+1}^t \gamma_{h,t''}$ . Note that we apply some form causal masking here: we take the key  $K_h \in \mathbb{R}^{D_a \times T}$  and value matrices  $V_h \in \mathbb{R}^{D_a \times T}$  with all the sequence timesteps and select the entries occurring before time  $t$ . The main difference with the usual causal mask  $(\mathbb{1}_{t' \leq t})_{t',t}$  is the inclusion of the forget factors. It can be efficiently computed leveraging partial products. We conclude by remarking that the same mask can be applied to softmax attention layers, applying it to the key-queries products before the softmax.

## A2 MESA LAYER BACKWARD COMPUTATION

### A2.1 MESA LAYER COMPUTATION BACKWARD PASS VIA SHERMAN-MORRISON

In this section, we detail how to compute the backward pass of the mesa layer with forget factor detailed in Section A1. Recall that the forward pass of the Mesa layer is computed recursively following

$$R_{h,t+1} = \gamma_{h,t+1}^{-1} \left( R_{h,t} - \frac{R_{h,t} k_{h,t+1} k_{h,t+1}^\top R_{h,t}}{\gamma_{h,t+1} + k_{h,t+1}^\top R_{h,t} k_{h,t+1}} \right) \quad (\text{A12})$$

$$\Delta e_{t,\text{mesa}} = \sum_{h=1}^H P_h V_h (M_{:,t} \odot K_h^\top \tilde{q}_{h,t}) \quad (\text{A13})$$

with  $R_{h,0} = \lambda_h I$ .

The forward pass can be decomposed into 3 steps:

1. First, the matrices  $R_{t,h}$  are computed sequentially.
2. Then, for all  $t$  and  $h$ , the transformed queries  $\tilde{q}_{h,t} = R_{h,t}q_{h,t}$  are computed.
3. Finally, using the transformed queries  $\tilde{Q}_h = (\tilde{q}_{h,t})_t$  as the queries, a standard cross-attention operation is computed from  $(V_h, K_h, \tilde{Q}_h)$  using the causal mask  $M$  that includes forgetting rates.

While the backward pass of 2 and 3 can be computed easily with automatic differentiation tools without much overhead compared to standard attention layers, the same thing cannot be said about 1. We will here discuss how the backward pass of the computation of  $\tilde{Q}_h$  can be computed in a memory-efficient way. Without loss of generality, we drop the subscript  $h$  for notational simplicity.

**The issue with automatic differentiation out of the box.** For all time  $t$ ,  $\tilde{q}_t = R_t q_t$  depends on  $q_t$ , but also  $K_t, \Gamma_t$  and  $\lambda$  through the variable  $R_t$ .

In the backward pass, we are given as input the gradient of the loss function w.r.t.  $\tilde{Q}$ , namely  $\frac{d\mathcal{L}}{d\tilde{q}_t}$  for all  $t$ . The goal is then to compute the gradient of the loss w.r.t. the input of  $\tilde{Q}$ , namely  $\frac{d\mathcal{L}}{dq_t}, \frac{d\mathcal{L}}{d\gamma_t}, \frac{d\mathcal{L}}{d\lambda}$ , which can be achieved via the chain rule.

While using automatic differentiation out of the box would take care of this computation, it would require in particular the storing of all intermediate variables  $R_t$ , which can be prohibitively expensive.

**Memory efficient custom backward pass.** Instead, we will show that storing the matrices  $K, \Gamma, Q$  as well as  $R_T$  where  $T$  is the last time step of the training sequence, is sufficient to exactly compute the backward pass. Indeed, given the aforementioned inputs, all  $R_t$  can be recomputed in linear complexity w.r.t.  $T$ , which means we can reconstruct recursively the inputs of  $\tilde{q}_t$  at all time steps.

By noticing that  $R_{t-1} = \gamma_t (R_t^{-1} - k_t k_t^\top)^{-1}$ , we can apply the Sherman-Morrison formula backwards to obtain  $R_{t-1}$  as

$$R_{t-1} = \gamma_t \left( R_t - \frac{R_t (-k_t) k_t^\top R_t}{1 + (-k_t)^\top R_t k_t} \right) \quad (\text{A14})$$

$$= \gamma_t \left( R_t - \frac{R_t k_t k_t^\top R_t}{k_t^\top R_t k_t - 1} \right) \quad (\text{A15})$$

We will now show how accumulating the right error signal and leveraging the vector-jacobian product trick together with automatic differentiation tools is sufficient for computing the full backward pass recursively.

Firstly, given the error signal and reconstructed  $R_t$  allows the computation of  $\frac{d\mathcal{L}}{dq_t}$  via

$$\frac{d\mathcal{L}}{dq_t} = \frac{d\mathcal{L}}{d\tilde{q}_t} \frac{d\tilde{q}_t}{dq_t} = \frac{d\mathcal{L}}{d\tilde{q}_t} S_t \quad (\text{A16})$$

Secondly, we rewrite  $\tilde{q}_t$  as a function of  $k_t, \gamma_t, R_{t-1}$  and  $q_t$ , i.e.

$$\tilde{q}_t = \mathcal{R}^{\text{forward}}(R_{t-1}, k_t, \gamma_t) q_t \quad (\text{A17})$$

Since  $\mathcal{L}$  depends on  $k_t$  only via both  $\tilde{q}_t$  and  $R_t$ , we can then rewrite

$$\frac{d\mathcal{L}}{dk_t} = \frac{d\mathcal{L}}{d\tilde{q}_t} \frac{d\tilde{q}_t}{dk_t} + \frac{d\mathcal{L}}{dR_t} \frac{dR_t}{dk_t} \quad (\text{A18})$$

$$= \frac{d\mathcal{L}}{d\tilde{q}_t} \frac{\partial \tilde{q}_t}{\partial k_t} + \frac{d\mathcal{L}}{dR_t} \frac{\partial R_t}{\partial k_t} \quad (\text{A19})$$

where, provided  $R_{t-1}, k_t, \gamma_t$  and  $q_t, \frac{\partial \tilde{q}_t}{\partial k_t}$  can be computed easily using e.g. automatic differentiation tools. Similarly, we have,

$$\frac{d\mathcal{L}}{d\gamma_t} = \frac{d\mathcal{L}}{d\tilde{q}_t} \frac{\partial \tilde{q}_t}{\partial \gamma_t} + \frac{d\mathcal{L}}{dR_t} \frac{\partial R_t}{\partial \gamma_t} \quad (\text{A20})$$

Notice that  $\frac{d\mathcal{L}}{dR_t}$  can be computed recursively following the chain rule

$$\frac{d\mathcal{L}}{dR_{t-1}} = \frac{d\mathcal{L}}{dR_t} \frac{\partial R_t}{\partial R_{t-1}} + \frac{d\mathcal{L}}{d\tilde{q}_t} \frac{\partial \tilde{q}_t}{\partial R_{t-1}} \quad (\text{A21})$$

where again, provided  $R_{t-1}, k_t, \gamma_t$  and  $q_t$ , both terms can be computed efficiently with standard automatic differentiation tools coupled with the well known vector-Jacobian product trick given the quantities  $\frac{d\mathcal{L}}{dR_t}$  and  $\frac{d\mathcal{L}}{d\tilde{q}_t}$ .

Thirdly, we can show that

$$\frac{d\mathcal{L}}{d\lambda} = \text{Tr} \left[ \frac{d\mathcal{L}}{dR_0} \right] \quad (\text{A22})$$

Combining everything, we can now implement the backward computation recursively via the following equations:

$$R_{t-1} = \gamma_t \left( R_t - \frac{R_t k_t k_t^\top R_t}{k_t^\top R_t k_t - 1} \right) \quad (\text{A23})$$

$$\frac{d\mathcal{L}}{dR_{t-1}} = \frac{d\mathcal{L}}{dR_t} \frac{\partial R_t}{\partial R_{t-1}} + \frac{\partial \mathcal{L}}{\partial \tilde{q}_t} \frac{\partial \tilde{q}_t}{\partial R_{t-1}} \quad (\text{A24})$$

$$\frac{d\mathcal{L}}{dk_t} = \frac{d\mathcal{L}}{d\tilde{q}_t} \frac{\partial \tilde{q}_t}{\partial k_t} + \frac{d\mathcal{L}}{dR_t} \frac{\partial R_t}{\partial k_t} \quad (\text{A25})$$

$$\frac{d\mathcal{L}}{d\gamma_t} = \frac{d\mathcal{L}}{d\tilde{q}_t} \frac{\partial \tilde{q}_t}{\partial \gamma_t} + \frac{d\mathcal{L}}{dR_t} \frac{\partial R_t}{\partial \gamma_t} \quad (\text{A26})$$

$$\frac{d\mathcal{L}}{dq_t} = \frac{d\mathcal{L}}{d\tilde{q}_t} R_t \quad (\text{A27})$$

$$\frac{d\mathcal{L}}{d\lambda} = \text{Tr} \left[ \frac{d\mathcal{L}}{dR_0} \right] \quad (\text{A28})$$

$R_T$  is assumed to be given and  $\frac{d\mathcal{L}}{dR_T} = 0$ . The above equations only require the storage of  $\frac{d\mathcal{L}}{dR_t}, \frac{d\mathcal{L}}{dR_{t-1}}, R_t, R_{t-1}$  at all time, and computes the backward pass in a similar time and memory complexity as for the forward pass. The derivation is identical without forgetting factors, by setting all  $\gamma$  to 1.

**Comment on runtime.** We highlight that, although this implementation of the mesa-layer reduces the memory footprint of the forward and backward pass substantially, the layer still runs forward (and backward) in time. This prevents the computation of all mesa-layer outputs in parallelization during training, a crucial advantage of softmax as well as linear attention. On the other hand, during test time, the mesa-layer benefits from the same advantages of linear self-attention or RNNs and predicts the next token without the necessity to store and attend to the past. In the next section, we present one potential avenue to improve the training time by approximating the necessary inversions by a Neumann series running in parallel.

## A2.2 ALTERNATIVE DERIVATION THROUGH THE IMPLICIT FUNCTION THEOREM

We here present an alternative way of deriving the gradients presented above that leverages the implicit function theorem. The key here is to remark that  $\hat{W}_t^{\text{mesa}}$  satisfies that the gradient of the least-square regression loss  $L$  is 0. For simplicity, we restrict ourselves to the case in which the output dimension of  $\hat{W}_t^{\text{mesa}}$  is one, that is  $\hat{W}_t^{\text{mesa}} = \hat{w}_t^\top$  for  $\hat{w}_t$  some column vector, and remark that we have to repeat the same operation over all rows of  $\hat{W}_t^{\text{mesa}}$  to obtain the full gradient, as all output coordinates are independent in the least-square regression problem. Therefore, we  $w$  defined through

the implicit function

$$\frac{dL}{dw}(\hat{w}_t) = \sum_{t'=1}^t M_{t',t}(\hat{w}_t^\top k_{t'} - v_{t'})k_{t'}^\top + \frac{M_{1,t}}{\lambda}\hat{w}_t^\top = 0. \quad (\text{A29})$$

We can then use the implicit function theorem and compute the derivative of  $w$  with respect to any quantity  $\cdot$  through

$$\frac{d\hat{w}_t}{d\cdot} = - \left( \frac{d^2 L_t}{dw^2}(w_t) \right)^{-1} \frac{d^2 L_t(\hat{w}_t)}{d\cdot dw} \quad (\text{A30})$$

$$= -R_t \frac{d^2 L_t(\hat{w}_t)}{d\cdot dw}. \quad (\text{A31})$$

For example, this yields

$$\frac{d\hat{w}_t}{dv_{t'}} = M_{t',t} R_t k_{t'}. \quad (\text{A32})$$

Finally, we can recover the desired gradient by combining the previous equation with the chain rule.

### A2.3 PARALLEL BACKWARD PASS THROUGH NEUMANN SERIES APPROXIMATION

*Note: We present this section for the sake of completeness – no experiments presented in this manuscript use this approximation.*

Although the previous custom backward gradient computation allows for dramatic memory savings during training, the underlying recursive least squares computation still suffers from linear scaling in time, similar to recurrent neural networks, as we cannot parallelize computation across time dimension.

Here, we discuss an alternative forward pass that can be used when one can afford storing all intermediate matrices  $R_{h,t}$  in time. This forward pass leverages a  $K$ -step truncated Neumann series to approximate the inverses in parallel, and is compatible with automatic differentiation tools out of the box. Interestingly, we can do this by simply repeating (with the same weights) a slightly altered linear self-attention layer  $K$  times.

Our goal is now to efficiently compute the terms  $\tilde{q}_t := R_t q_t = (K_t K_t^\top + \frac{1}{\lambda} I)^{-1} q_t$  for all time steps in parallel. Indeed, once given these vectors, one can leverage Equation A11 and efficient dot-product attention (DPA) layers implementations<sup>2</sup>. Note that we here ignore the forgetting factors, but their partial products can easily be integrated in one of the  $K_t$  in  $K_t K_t^\top$  to recover the version with forget rates described above.

Given an invertible matrix  $X$  with operator norm less than 1, the truncated Neumann series approximates its inverse by

$$X^{-1} \approx \tilde{X}_{(K)}^{-1} := \sum_{k=0}^{K-1} (I - X)^k. \quad (\text{A33})$$

When multiplying a vector from the right, we see that

$$\tilde{x}^{(K)} := \tilde{X}_{(K)}^{-1} x = \sum_{k=0}^{K-1} (I - X)^k x \quad (\text{A34})$$

$$= \sum_{k=1}^K (I - X)^k x + x \quad (\text{A35})$$

$$= (I - X) \sum_{k=0}^{K-1} (I - X)^k x + x \quad (\text{A36})$$

$$= (I - X) \tilde{x}^{(K-1)} + x \quad (\text{A37})$$

<sup>2</sup>See [https://flax.readthedocs.io/en/latest/\\_modules/flax/linen/attention.html](https://flax.readthedocs.io/en/latest/_modules/flax/linen/attention.html) for an implementation of DPA in JAX (Bradbury et al., 2018).

An advantage of the truncated Neumann series compared to other approximate inverse techniques such as Newton-Iteration is that we can compute more series elements without passing intermediate matrices across algorithmic steps – which in turn makes it memory efficient and straightforward to use in the light of automatic differentiation. We only need to keep the original matrix we wish to invert in memory at all times and store the intermediate vectors  $\tilde{x}^{(k)}$  for the backward pass.

We now look at the quantities we wish to compute, that is  $\tilde{q}_t = (K_t K_t^\top + \frac{1}{\lambda} I)^{-1} q_t$ , and approximate it by  $\tilde{q}_t^{(K)}$ , obtained by multiplying  $q_t$  to the  $K$ -step truncated Neumann series approximating the inverse term  $(K_t K_t^\top + \frac{1}{\lambda} I)^{-1}$ . Note that a normalization by the operator norm of the matrix inside the inverse is necessary for the approximation to hold.

Then,  $\tilde{q}_t^{(K)}$  can be computed recursively as

$$\tilde{q}_t^{(k+1)} = \left( I - \left( K_t K_t^\top + \frac{1}{\lambda} I \right) \right) \tilde{q}_t^{(k)} + q_t \quad (\text{A38})$$

$$= q_t + \left( 1 - \frac{1}{\lambda} \right) \tilde{q}_t^{(k)} - K_t K_t^\top \tilde{q}_t^{(k)} \quad (\text{A39})$$

and thus by denoting  $\tilde{Q}_t^{(k)} := (\tilde{q}_{t'}^{(k)})_{t'=1}^t$ , we have

$$\tilde{Q}_{k+1}^{(k+1)} = Q_t + \left( 1 - \frac{1}{\lambda} \right) \tilde{Q}_t^{(k)} - K_t K_t^\top \tilde{Q}_t^{(k)} \quad (\text{A40})$$

which is the sum of simple terms with a DPA computed between  $K_t, K_t, \tilde{Q}_t^{(k)}$ .

After obtaining  $\tilde{Q}_t^{(K)}$  to approximate  $\tilde{Q}_t$ , we compute the approximate least-squares solution as described above. Note that other implementations could save us from effectively recomputing  $(K_t K_t^\top)$  at every iteration of Equation A40 by simply pre-computing these terms before running the Neumann approximation. We nevertheless observe the former version to be faster when timing for forward and backward computation and speculate the reason being the highly optimized implementation of DPA as the backbone of the self-attention layer. Note that a simple byproduct of the derivations here is the insight that chaining linear self-attention layers can actually easily implement truncated Neumann series computation – especially if the goal is an inverse multiplied by a known vector. See Section A4.2 for a more in-depth analysis.



### A3 VISUALIZATION OF WEIGHTS AND ATTENTION MAPS OF TRAINED TRANSFORMERS

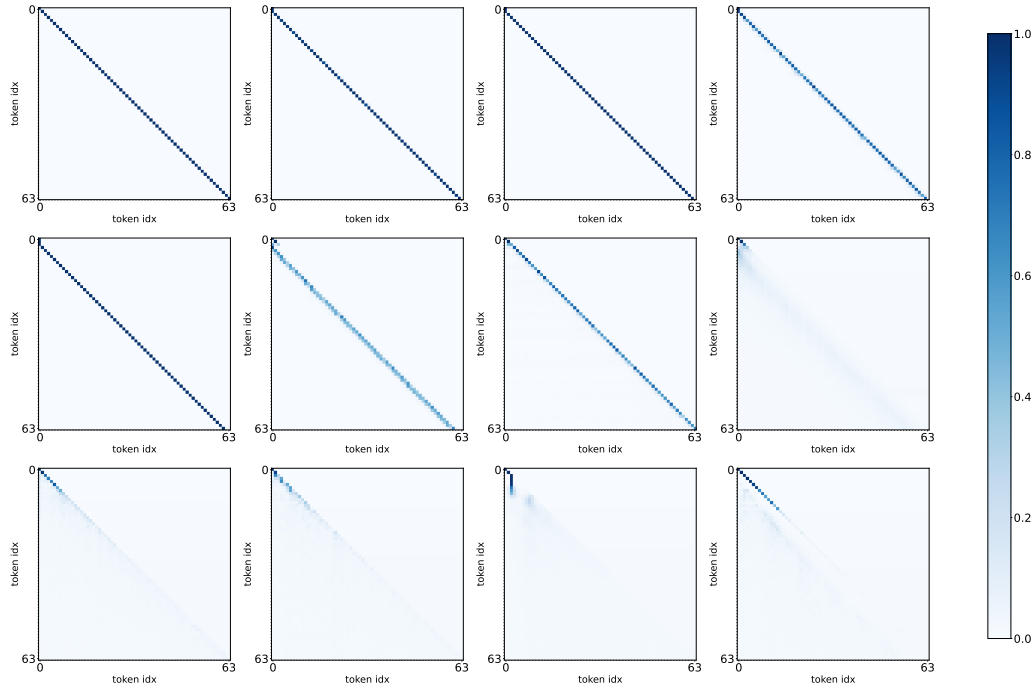


Figure A1: **Softmax attention maps of the 2-layer softmax-only Transformer trained on the Pile.** We average the attention maps of the first softmax-attention layer over a batch of size 256 and observe stable off diagonals with different offsets and widths indicating clean copying behavior based on positional encodings in multiple heads.

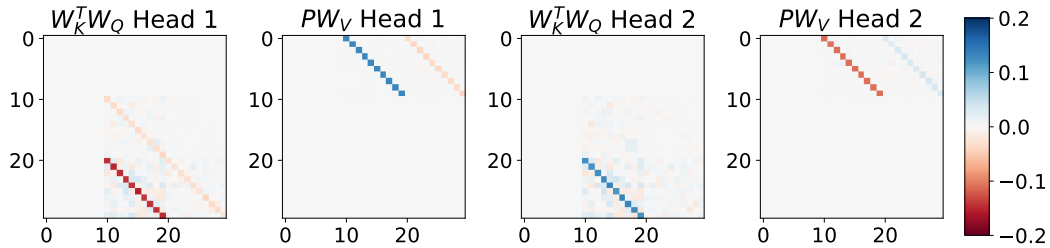


Figure A2: **Mesa-optimization in a trained linear self-attention layer.** We inspect the parameters of a two-headed, linear self-attention layer trained to predict the future state of a linear dynamical system. The dominant pattern obtained after learning corresponds to our mesa-gradient descent construction described in Section 3. The faint additional structure can be further reverse-engineered, and results from a modified mesa-objective function, Eq. A43, discovered by base-optimization of Eq. 10. Please compare to the similar structure of the weight matrix products of our construction.

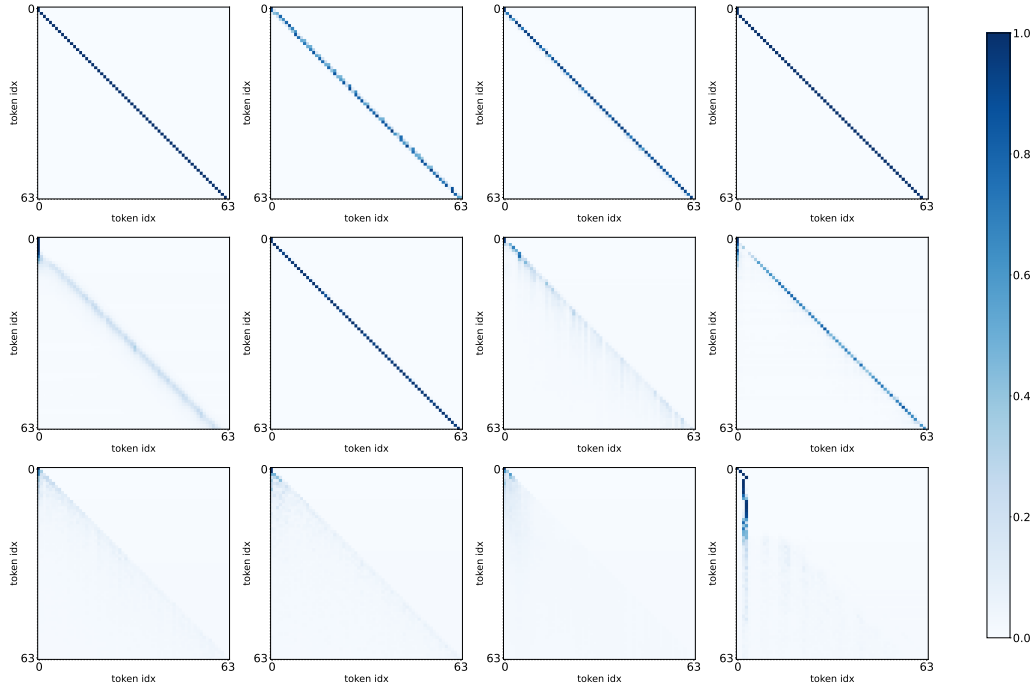


Figure A3: **Softmax attention maps of the 2-layer mesa-hybrid trained on the Pile.** We average the attention maps of the first layer i.e. a softmax self-attention layer over a batch of size 256 and observe stable off diagonals with different offsets and widths indicating clean copying behavior based on positional encodings in multiple heads.

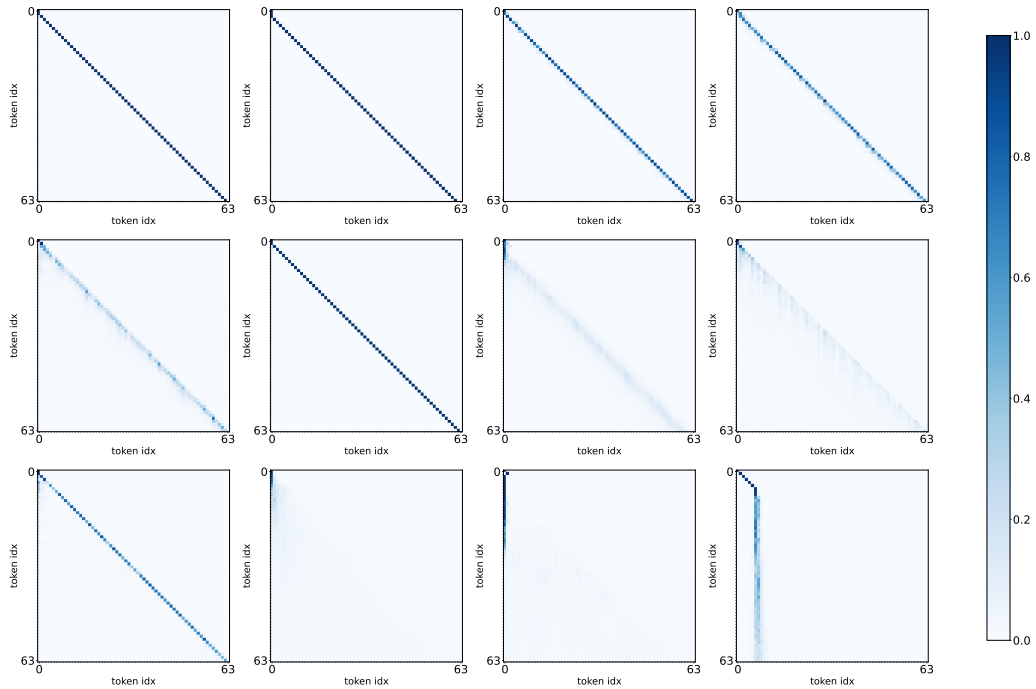


Figure A4: **Softmax attention maps of the 2-layer linear-hybrid trained on the Pile.** We average the attention maps of the first layer i.e. a softmax self-attention layer over a batch of size 256 and observe stable off diagonals with different offsets and widths indicating clean copying behavior based on positional encodings in multiple heads.

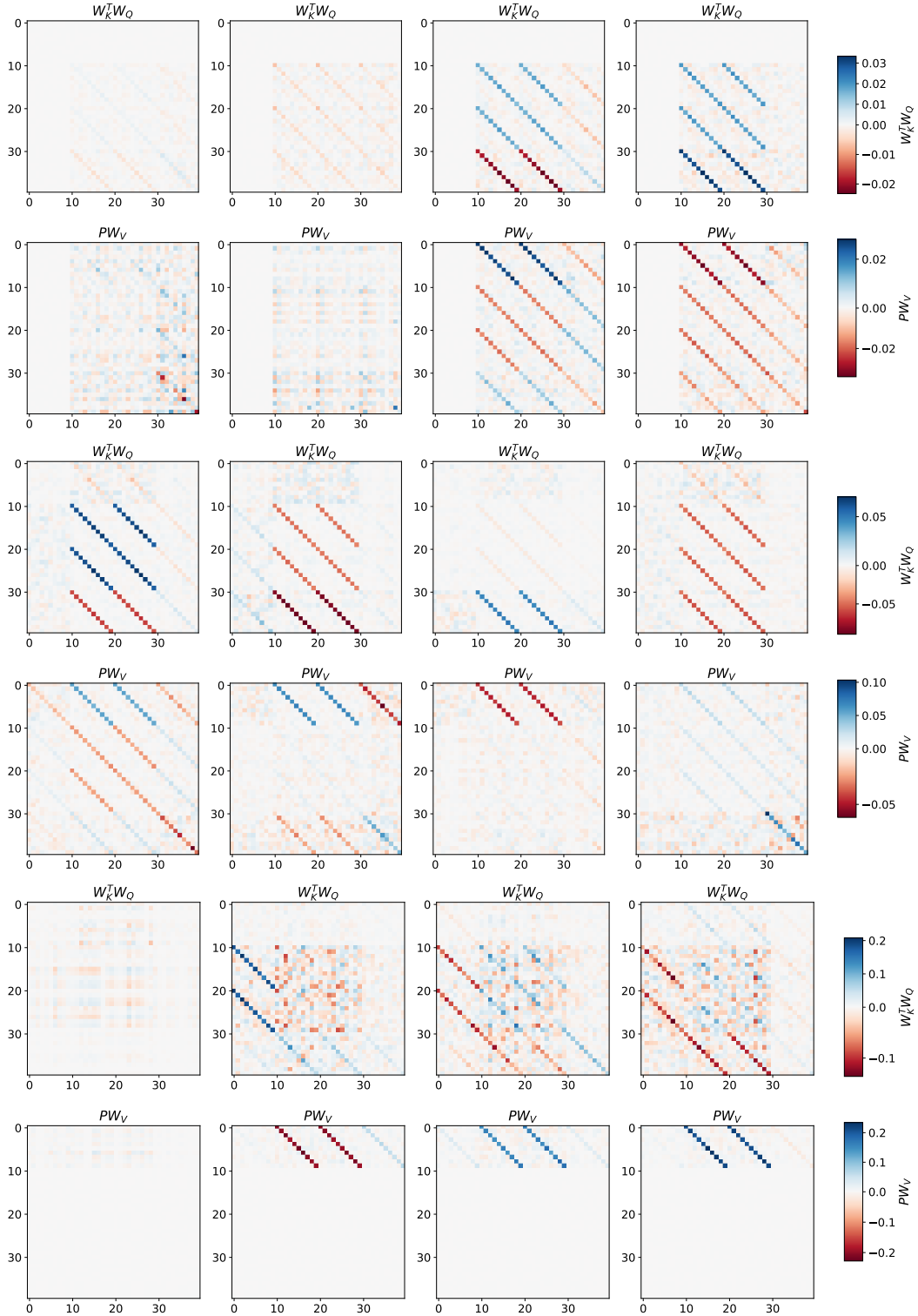


Figure A5: **Weights of the deep 6-layer linear Transformers trained on constructed tokens**  $e_t = (0, s_t, s_t, s_{t-1})$ . We observe clear structure in the trained Transformer weight products  $W_K^\top W_Q$  as well as  $PW_V$ . Note that this structure seems to be sufficient to approximate  $(S_{t-1}S_{t-1}^\top + 1/\lambda I)^{-1}s_t$ , see probing experiment in the main text, Section A2.3 and Section A4. We show here all 4 heads (f.l.t.r.) of the first (top 2 rows), the second (next 2 rows), and the last (last 2 rows) linear layer.

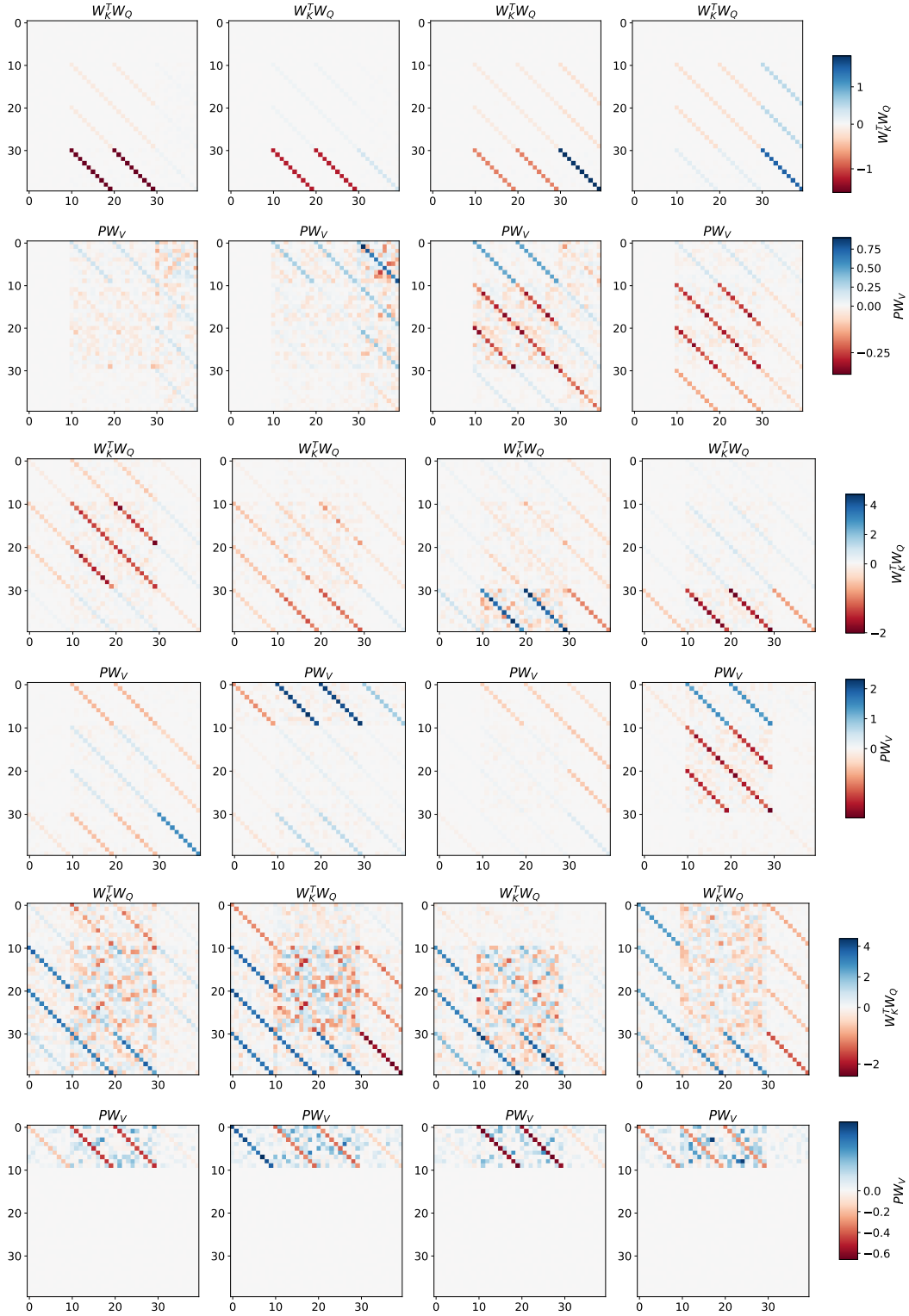


Figure A6: **Weights of the deep 6-layer softmax Transformers trained on constructed tokens**  $e_t = (0, s_t, s_t, s_{t-1})$ . We observe a lot of structure in the trained Transformer weight products  $W_K^T W_Q$  as well as  $PW_V$ . Note that this structure seems to be sufficient to approximate  $(S_{t-1} S_{t-1}^T + 1/\lambda I)^{-1} s_t$ , see probing experiment in the main text, Section A2.3 and Section A4. We show here all 4 heads (f.l.t.r.) of the first (top 2 rows), the second (next 2 rows), and the last (last 2 rows) softmax layer.

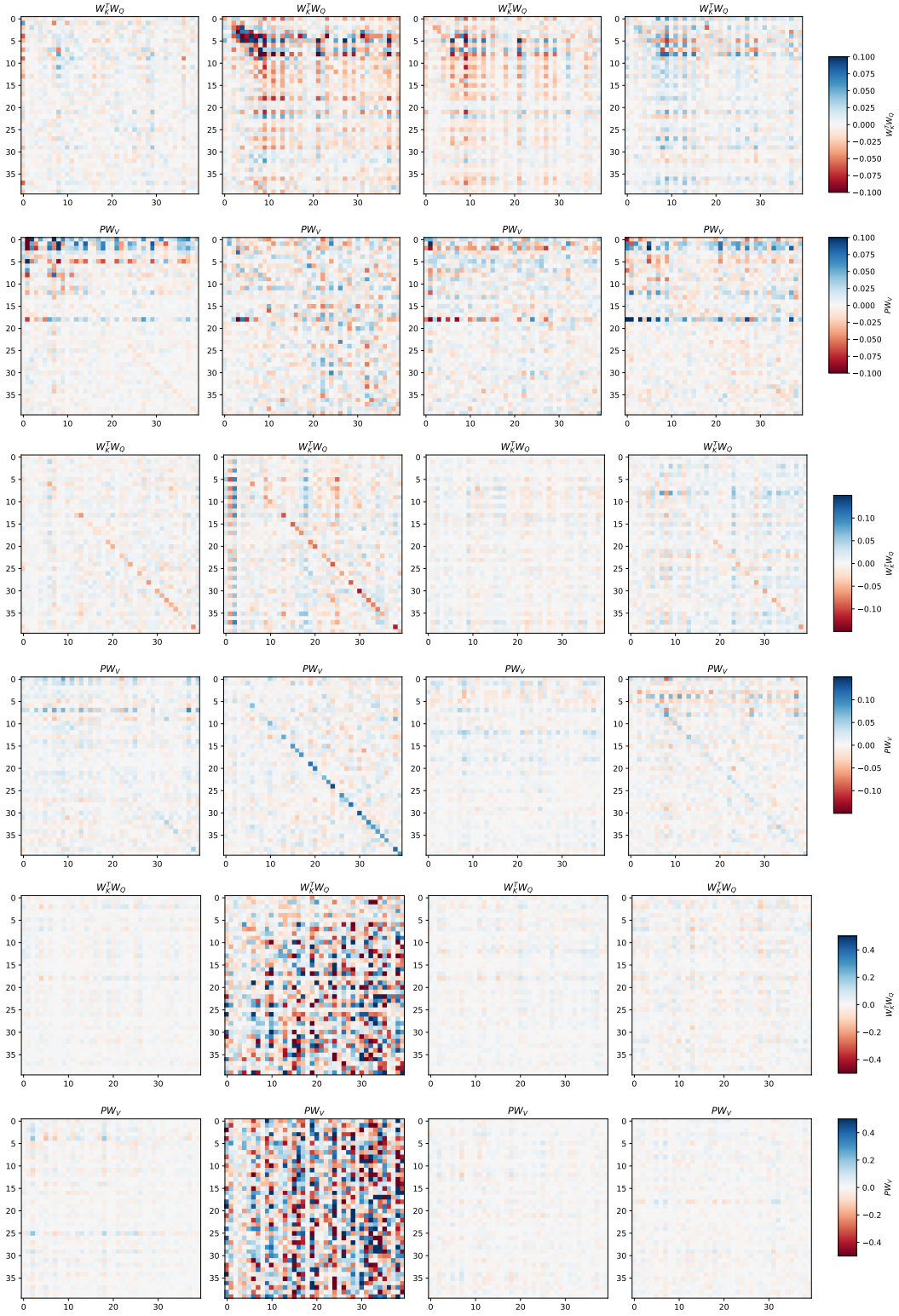


Figure A7: **Weights of the deep 1+6-layer linear-hybrid Transformers trained on unconstructed tokens  $e_t = s_t$ .** We observe some diagonal structure in the trained Transformer weight products  $W_K^T W_Q$  as well as  $PW_V$ . Note that this structure seems to be sufficient to approximate  $(S_{t-1} S_{t-1}^T + 1/\lambda I)^{-1} s_t$ , see probing experiment in the main text, Section A2.3 and Section A4. We show here all 4 heads (f.l.t.r.) of the first (top 2 rows), the second (middle 2 rows) and last (last 2 rows) linear layer after the first softmax layer.

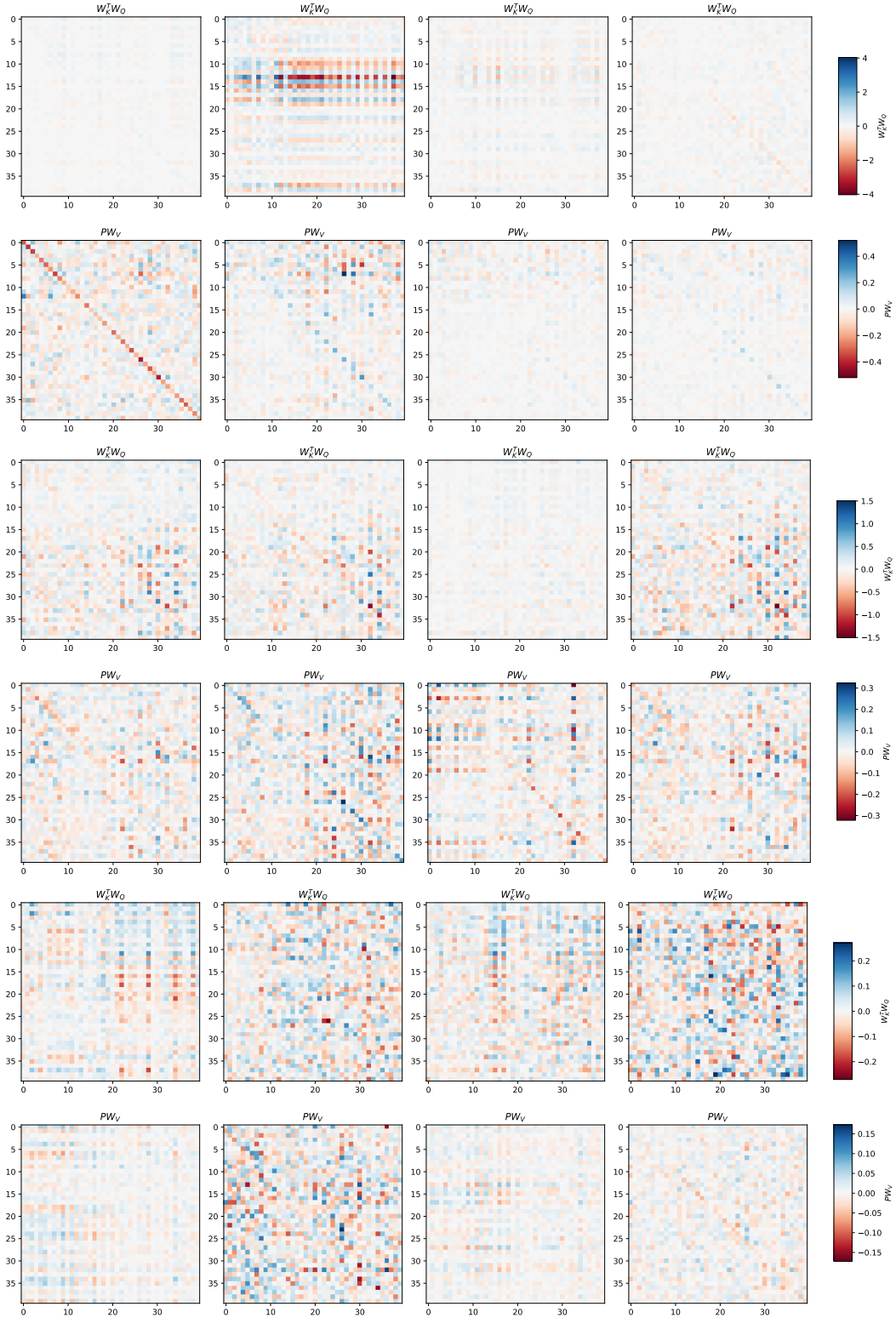


Figure A8: **Weight products of the deep 7-layer softmax Transformers trained on unconstructed tokens**  $e_t = s_t$ . We observe some diagonal structure in the trained Transformer weight products  $W_K^\top W_Q$  as well as  $PW_V$ . Note that this structure seems to be sufficient to approximate layer-wise the final prediction  $s_{t+1}$  as well as  $(S_{t-1}S_{t-1}^\top + 1/\lambda I)^{-1}s_t$ , see probing experiment in the main text, Section A2.3 and Section A4. We show here all 4 heads (f.l.t.r.) of the second (top 2 rows) the third (middle 2 rows) and the last (last 2 rows) layers after the first (potential) copying-softmax-layer.

## A4 MECHANISTIC INTERPRETABILITY OF TRANSFORMERS TRAINED ON LINEAR DYNAMICS

### A4.1 SINGLE-LAYER MESA-GRADIENT DESCENT

We state here for completion the training objective of Transformers trained on sequences with initial state  $s_1 \sim \mathcal{N}(0, I)$  with subsequent states  $t = 1, \dots, T$  generated according to the rule  $s_t = W^* s_{t-1} + \epsilon_t$ , where  $\epsilon_t \sim \mathcal{N}(0, \sigma_s^2 I)$  introduces uncorrelated Gaussian noise. We take  $W^*$  to be a random orthogonal matrix. The Transformer models  $t_\theta$  are trained by stochastic online minimization of the autoregressive loss  $\mathcal{L}(\theta)$ , cf. Eq. 10.

After training, we obtain structured matrix products  $W_K^\top W_Q, PW_V$  per layer which we visualize in Figure A2 for a single linear self-attention Transformer and in Figure A5 for the multi-layer case. When inspecting the trained weight matrix products, one observes stable values across block-diagonals of the input size across all layers.

We start by analyzing the simpler single layer Transformer computation and reduce it to

$$\begin{aligned} e_t &\leftarrow e_t + \text{LSA}(e_t; (e_{t'})_{t'=1}^t) \\ &= \sum_{h=1}^H \phi_1^t(d_h^{PV}, d_h^{K^T Q})_{s_t} + \phi_2^t(d_h^{PV}, d_h^{K^T Q})_{s_{t-1}}, \end{aligned} \quad (\text{A41})$$

where  $\text{LSA}(e_t; (e_{t'})_{t'=1}^t)$  denotes the linear self-attention operation with context  $(e_{t'})_{t'=1}^t$  and query  $e_t$ , and with  $d$  inputs to the functions  $\phi$  defined as follows:

$$\begin{aligned} \phi_M^t(d^{PV}, d^{K^T Q}) &= \sum_{t'=1}^t d^{K^T Q_{M1}} \cdot (d^{PV_1} s_{t'} s_{t'}^\top + d^{PV_2} s_{t'-1} s_{t'}^\top) \\ &\quad + d^{K^T Q_{M2}} \cdot (d^{PV_1} s_{t'} s_{t'-1}^\top + d^{PV_2} s_{t'-1} s_{t'-1}^\top). \end{aligned}$$

Here  $d^{PV}, d^{K^T Q}$  corresponds to the 4 (the lower right square of size  $2d \times 2d$  of  $K^T Q$ ) resp. 2 (the upper right rectangle of size  $d \times 2d$  of  $PV$ ) non-zero off-diagonal values that we observe

in the trained weight products per head i.e.  $W_k^\top W_q = \begin{pmatrix} \cdot & \cdot \\ \cdot & d^{K^T Q_{1,1}} I_s & d^{K^T Q_{1,2}} I_s \\ \cdot & d^{K^T Q_{2,1}} I_s & d^{K^T Q_{2,2}} I_s \end{pmatrix}$  as well as

$$PW_v = \begin{pmatrix} \cdot & d^{PV_1} I_s & d^{PV_2} I_s \\ \cdot & \cdot & \cdot \\ \cdot & \cdot & \cdot \end{pmatrix}.$$

We extract the values from the trained models by computing the mean of the block diagonal matrices. Note that we allow for all combinations between temporally accumulated block matrices and the current token inputs  $e_t = [0, 0, s_t, s_{t-1}]^\top$  with specific strengths controlled through the parameters. In all of our experiments, we observe a performance increase when changing from single-head to two-head attention layers (more than two heads do not alter performance). This can be explained by the improved flexibility of scaling the different terms individually as can be seen by comparing the formulas for one and two heads.

Following equation A41, the prediction of a two-head single layer Transformer with our construction of  $e_t = [0, s_t, s_{t-1}]$  is given by

$$\begin{aligned} \hat{s}_{t+1} &= 0 + \sum_{h=1}^2 \phi_1^t(d_h^{PV}, d_h^{K^T Q})_{s_t} + \phi_2^t(d_h^{PV}, d_h^{K^T Q})_{s_{t-1}} \\ &= \underbrace{\left( \phi_1^t(d_1^{PV}, d_1^{K^T Q}) + \phi_1^t(d_2^{PV}, d_2^{K^T Q}) \right)}_A s_t + \underbrace{\left( \phi_2^t(d_1^{PV}, d_1^{K^T Q}) + \phi_2^t(d_2^{PV}, d_2^{K^T Q}) \right)}_B s_{t-1} \end{aligned}$$

with

$$\begin{aligned}
A &= \sum_{t'=1}^t d_1^{K^T Q_{11}} \cdot \left( d_1^{PV_1} s_{t'} s_{t'}^\top + d_1^{PV_2} s_{t'-1} s_{t'}^\top \right) + d_1^{K^T Q_{12}} \cdot \left( d_1^{PV_1} s_{t'} s_{t'-1}^\top + d_1^{PV_2} s_{t'-1} s_{t'-1}^\top \right) \\
&\quad + d_2^{K^T Q_{11}} \cdot \left( d_2^{PV_1} s_{t'} s_{t'}^\top + d_2^{PV_2} s_{t'-1} s_{t'}^\top \right) + d_2^{K^T Q_{12}} \cdot \left( d_2^{PV_1} s_{t'} s_{t'-1}^\top + d_2^{PV_2} s_{t'-1} s_{t'-1}^\top \right) \\
&= \sum_{t'=1}^t \lambda_{A,1} s_{t'} s_{t'}^\top + \lambda_{A,2} s_{t'-1} s_{t'}^\top + \lambda_{A,3} s_{t'} s_{t'-1}^\top + \lambda_{A,4} s_{t'-1} s_{t'-1}^\top. \tag{A42}
\end{aligned}$$

after summarizing by combining factors in front of the same outerproducts. (B) is computed accordingly. Here, every outer product combination of  $s_{t'}$  and  $s_{t'-1}$ , is weighted by a product of two factors, before summarizing, that are co-dependent within one head. Therefore we indeed need a minimum of two heads to obtain independent  $\lambda_i$ . However, adding further heads does not increase performance as no further expressivity is gained. See for a visualization of the corresponding weight matrix products and factors that we extract from the block diagonals Figure A2. The extracted mean values of our trained Transformer block diagonals are reported in Table A1.

Table A1: Understanding the algorithm parametrization of Transformers trained on linear dynamics. To test the significance of the  $\lambda$  values derived in Eq. A42, we set almost all values i.e.  $\lambda_{\cdot,1} = \lambda_{\cdot,2} = \lambda_B = 0$  - we call this loss  $\mathcal{L}_{\text{reduced}}$ . This coincides as shown to gradient descent on a meta-learned initial prediction and learning rate (see Eq. A43). To show the influence of the  $\lambda$  values corresponding to GD, we compute the algorithms performance when only setting  $\lambda_{A,3/4} = 0$  and observe a drastic loss increase, we denote this loss as  $\mathcal{L}_{\text{ablation}}$  and also report the loss of one step of GD as  $\mathcal{L}_{\text{GD}}$ .

Seed	$\lambda$	$\lambda_{\cdot,1}$	$\lambda_{\cdot,2}$	$\lambda_{\cdot,3}$	$\lambda_{\cdot,4}$	$\mathcal{L}$	$\mathcal{L}_{\text{reduced}}$	$\mathcal{L}_{\text{ablation}}$	$\mathcal{L}_{\text{GD}}$
1	$\lambda_A$	0.000620	0.000254	-0.033142	0.000149	0.8923	0.9007	1.7275	0.9151
1	$\lambda_B$	0.003644	0.000034	-0.000978	-0.000129				
2	$\lambda_A$	-0.001648	0.000089	-0.033428	0.001809	0.8926	0.9039	1.7349	0.9088
2	$\lambda_B$	0.003974	-0.000215	-0.000423	0.000023				
3	$\lambda_A$	-0.003381	0.000776	-0.033751	0.006270	0.8941	0.9408	1.7643	0.9088
3	$\lambda_B$	0.002756	-0.000444	-0.002846	0.000625				
4	$\lambda_A$	0.001905	0.000270	-0.033858	-0.002946	0.8928	0.9089	1.7417	0.9019
4	$\lambda_B$	0.003851	0.000285	0.000873	0.000225				
5	$\lambda_A$	-0.001676	0.000324	-0.033557	0.001557	0.8932	0.9050	1.7222	0.9136
5	$\lambda_B$	0.002450	-0.000028	-0.000027	0.000441				

We now aim to interpret this parametrized algorithm and motivate it by gradient descent on a particular regression loss. Since the parametrizations remain constant across a sequence, we speculate that the Transformer has two principles by which it aims to predict the next token: gradient descent, and past-token averaging. The latter becomes especially useful for quickly contracting dynamics after convergence since simply copying over the last token can be one optimal and simple-to-implement solution, see Section A5, even when aiming to obtain low loss on the entire sequence. We thus hypothesize that past-token averaging is a simple way to overcome the sub-optimality of taking only one step of gradient descent.

Consider again the squared error loss from Eq. 3, which we hypothesize is internally optimized inside a single layer of self-attention

$$L_t^{\text{self-attention}}(W) = \frac{1}{2} \sum_{t'=1}^{t-1} \|s_{t'} - W s_{t'-1}\|^2,$$

We now compute and evaluate the gradient of the loss evaluated at the initial  $W = \tilde{\lambda}_1 I$  leading to an initially scaled prediction of the current  $s$  i.e.  $\hat{s}_{t+1} = \tilde{\lambda}_1 s_t$ ,

$$\nabla_W L_t^{\text{self-attention}}(\tilde{\lambda}_1 I) = - \sum_{t'=1}^{t-1} (s_{t'} - \tilde{\lambda}_1 s_{t'-1}) s_{t'-1}^\top.$$



The prediction after a gradient step can be computed by

$$\begin{aligned}
\hat{s}_{t+1} &= (\tilde{\lambda}_1 I - \eta_1 \nabla_W L_t^{\text{self-attention}}) s_t \\
&= \tilde{\lambda}_1 s_t - \eta_1 \sum_{t'=1}^{t-1} (s_{t'} - \tilde{\lambda}_1 s_{t'-1}) s_{t'-1}^\top s_t \\
&= \tilde{\lambda}_1 s_t + \left( \sum_{t'=1}^{t-1} \lambda_{C,3} s_{t'} s_{t'-1}^\top + \lambda_{C,4} s_{t'-1} s_{t'-1}^\top \right)^\top s_t. \tag{A43}
\end{aligned}$$

Note that this is a stripped down version of the derivation above, see equation A42. We now simply compare the final MSE loss when setting  $\lambda_{A,1} = \lambda_{A,2} = \lambda_B = 0$  and observe minimal loss degradation, see Table A1. Given this robustness, we are confident that almost all of the behavior and performance of the trained Transformer in this setting can be explained by simply descending the mesa-objective of Eq. 3 by gradient descent. We also see that empirically using an initial prediction and therefore a non-zero implicit initial weight has some influence on the final performance. Note that in certain settings the transformer can obtain a significantly improved performance when including the other terms in A42, as well, as can be seen in A5. Furthermore, note that to realize full expressivity in  $\lambda_{A,3} = \lambda_{A,4}$  it requires 6 parameters coming from both heads.

#### A4.2 MULTI-LAYER ACCELERATED MESA-GRADIENT DESCENT

We now return to the mesa-optimization algorithms presented in Section 3 – stacked mesa-gradient descent layers, and preconditioned mesa-gradient descent – and present them in full detail, in the context of the linear dynamics prediction problems studied in the main text.

**Review:  $d$ -layers of self-attention can implement  $d$  steps of gradient descent in the few-shot setting.** We start by repeating the multi-layer construction provided in von Oswald et al. (2023) which allows a Transformer, without causal masking, and applied to the few-shot regression setting. This construction performs a gradient descent step per layer while simultaneously constructing a prediction on some final input. Compared to Section 2, we slightly change notation to easily bridge the gap to the autoregressive case in the next paragraph. Recall the squared error regression loss given  $T - 1$  data pairs  $(s_{t'}, s_{t'+1})$

$$L(W^{(0)}) = \frac{1}{2} \sum_{t'=1}^{T-1} (W^{(0)} s_{t'} - s_{t'+1})^2,$$

with the gradient given by

$$\nabla_W L(W^{(0)}) = \sum_{t'=1}^{T-1} (W^{(0)} s_{t'} - s_{t'+1}) s_{t'}^\top$$

inducing a change in the weights  $\Delta W^{(0)} = -\eta \nabla_W L(W^{(0)})$ . We now evaluate the the loss again at  $W^{(1)} = W^{(0)} + \Delta W^{(0)}$ :

$$\begin{aligned}
L(W^{(1)}) &= L(W^{(0)} + \Delta W^{(1)}) = \frac{1}{2} \sum_{t'=1}^{T-1} ((W^{(0)} + \Delta W^{(1)}) s_{t'} - s_{t'+1})^2 \\
&= \frac{1}{2} \sum_{t'=1}^{T-1} (W^{(0)} s_{t'} - (s_{t'+1} - \Delta W^{(1)}))^2 \\
&= \frac{1}{2} \sum_{t'=1}^{T-1} (W^{(0)} s_{t'} - \tilde{s}_{t'+1}^{(1)})^2
\end{aligned}$$

with  $\tilde{s}_{t'+1}^{(1)} = s_{t'+1} - \Delta W^{(1)}$ . Note that when repeating this algorithm, we descend the regression loss after  $d$  steps of gradient descent by *transforming* the targets instead of updating the weights. Note that we are here not learning weights which we could use for test predictions. Nevertheless, when using the induced target transformation on some novel data point  $s_{T+1}$  while simultaneously transforming the targets of our dataset, we see that after a  $-1$  correction i.e.  $\hat{s}_{T+1} = W^{(0)} s_{T+1} +$

$-1 \sum_{l=0}^{d-1} -\Delta W^{(d)}_{s_{T+1}} = W^{(d)}_{s_{T+1}}$ , we obtain an equivalent prediction to the one of standard gradient descent. Note that the linear self-attention weight matrices provided in the main text for the single-step case directly implement this multi-step case when we restrict the attention to the first  $T - 1$  datapoints.

To implement this  $d$ -step algorithm in a Transformer, if all bias terms are zero,  $W_k^\top W_q = \begin{pmatrix} 0 & 0 \\ 0 & I_s \end{pmatrix}$ , and  $PW_v = \begin{pmatrix} -\eta I_s & \eta W_0 \\ 0 & 0 \end{pmatrix}$ , and the token at initialization is  $e_t^{(0)} = (s_{t+1}, s_t)$  for the training data and  $e_{T+1}^{(0)} = (-W_0 s_{T+1}, s_{T+1})$  for the test point, after  $d$  such layers, the last token in which we compute the test data prediction is transformed into  $e_{T+1}^{(d)} = (-W_0 s_{T+1} + \sum_{l=0}^{d-1} -\Delta W^{(d)}_{s_{T+1}}, s_{T+1})$ . The  $y$ -component of this token contains again the (negative) of the prediction obtained by a linear model that underwent  $d$  steps of gradient descent. Therefore, configured as such, our  $d$  self-attention layers take  $d$  steps of mesa-gradient descent toward solving a least-squares problem. Note that in this construction the lower half of the tokens  $e_t^{(l)} = (\cdot, s_t) \forall l$  keep unchanged throughout the Transformer forward pass.

**$d$ -layers of causally-masked self-attention can implement  $d$  steps of *online* gradient descent.**

To transfer the previous multi-layer construction to the autoregressive setting, we make two observations: (i) we now wish to make a prediction at every time step which will require more token space, and (ii) introducing causal masking will affect the computations carried out by the layer of von Oswald et al. (2023) reviewed above, leading to  $T$  different models learned in parallel by an unusual variant of gradient descent.

To see (i), we note that at every point in time the Transformer needs to keep in memory throughout its forward pass not only the inputs but also the targets,  $(s_{t'}, s_{t'+1})$  for  $t' \in \{1, \dots, T\}$ . This is the case as we need both to transform some target  $s_{t'}$  through gradient descent dynamics to implicitly keep updating the learned linear model, but also to use that same target  $s_{t'}$  now as input to the implicitly learned model to construct a final output. This observation motivates the token construction  $e_t = (-W_0 s_t, s_t, s_t, s_{t-1})$ , where the last two entries are kept unchanged throughout the Transformer forward pass. This token construction suggests the following weight configuration for a 2-headed linear self-attention layer:

$$\begin{aligned} W_{k,1}^\top W_{q,1} &= \begin{pmatrix} 0 & 0 & 0 & 0 \\ 0 & 0 & 0 & 0 \\ 0 & 0 & 0 & 0 \\ 0 & 0 & I_s & 0 \end{pmatrix}, \\ P_1 W_{v,1} &= \begin{pmatrix} 0 & -\eta I_y & 0 & \eta W_0 \\ 0 & 0 & 0 & 0 \\ 0 & 0 & 0 & 0 \\ 0 & 0 & 0 & 0 \end{pmatrix}, \\ W_{k,2}^\top W_{q,2} &= \begin{pmatrix} 0 & 0 & 0 & 0 \\ 0 & 0 & 0 & 0 \\ 0 & 0 & 0 & 0 \\ 0 & 0 & 0 & I_s \end{pmatrix}, \\ P_2 W_{v,2} &= \begin{pmatrix} 0 & 0 & 0 & 0 \\ 0 & -\eta I_y & 0 & \eta W_0 \\ 0 & 0 & 0 & 0 \\ 0 & 0 & 0 & 0 \end{pmatrix}. \end{aligned}$$

The dynamics induced by these two heads are equivalent but are *evaluated* in head 1 at the current  $s_{t'}$  which we use to make the next token prediction and at 2 at the training data input  $s_{t'-1}$ , to change the moving targets based on our previously discussed gradient-based transformation of the targets.

Given these weights in layer  $l$ , we obtain the following change in the tokens

$$\begin{aligned} e_{t+1} &= e_t + \Delta e_t^{(l)} = (\hat{s}_{t+1}^{(l)}, \tilde{s}_t^{(l)}, s_t, s_{t-1}) + (-\Delta W_t^{(l)} s_t, -\Delta W_t^{(l)} s_{t-1}, 0, 0) \\ &= (\hat{s}_{t+1}^{(l)}, \tilde{s}_t^{(l)}, s_t, s_{t-1}) + (\Delta \hat{s}_{t+1}^{(l)}, \Delta \tilde{s}_t^{(l)}, 0, 0) \end{aligned}$$

with  $\Delta W_t^{(l)} = -\eta \sum_{t'=1}^t (W_0 s_{t'-1} - \tilde{s}_{t-1}^{(l)}) s_{t'-1}^\top$  and  $\hat{s}_{t+1}^{(0)} = -W_0 s_t$ ,  $\tilde{s}_t^{(0)} = s_t$ . Note that now in the causally-masked setting, the sum only runs to element  $t$  for the token  $e_t$  and that therefore the transformed targets each follow their own dynamics instead of the gradient summed across the sequence, as in the few-shot regression case. The above construction is equivalent to the few-shot setting, for which we would want to make a prediction based on  $d$  steps of gradient descent for the test as well as the training data, i.e., at all points in time.

Furthermore, we can motivate this token update as the gradient of the time-dependent loss  $L_t(W_0) = \frac{1}{2} \sum_{t'=1}^t (W_0 s_{t'-1} - \tilde{s}_{t-1}^{(l)})^2$  for which again the targets at time step  $t$  change throughout the layers based on their specific target transformation mechanism. This online gradient descent algorithm was proved to be sub-optimal w.r.t. conventional (full-batch) gradient descent by Ding et al. (2023). They show that, in the limit of infinitely many layers, this construction implements online gradient descent, which does not coincide with the optimal (recursive) least-squares solution. Additionally, stochastic gradient descent with non-vanishing learning rates does not converge so the effective weight does not converge to the optimal solution when given infinitely many samples.

In the next section we will show how, at least in theory, multi-layer self-attention can implement a different algorithm which can lead to the desired result, even in the causally-masked setting. We end by noting that the aforementioned weight construction, despite being potentially sub-optimal, motivates our token construction  $e_t = (0, s_t, s_t, s_{t-1})$  which we use throughout all experiments when training deep Transformers, i.e., whenever the model has more than one self-attention layer. Note that  $-W_0 s_t = 0$  since we assume an  $W_0 = 0$ . Finally, we stress that until now it is not clear how to incorporate common  $L2$  regularization into the (online) gradient descent dynamics. This however is now in the autoregressive case of particular importance: In the beginning of the sequence the causally masked Transformer is forced to solve an under-constrained learning problem, dependent on the input data dimension and data generation. The following paragraph will again provide a simple solution to this problem.

**$d$ -layers of causally-masked self-attention can approximate optimal preconditioned gradient descent.** Our results are influenced by the GD++ algorithm presented by von Oswald et al. (2023), which can lead to accelerated optimization by applying a whitening transform to input data. We restate the goal of the autoregressive Transformer, namely, to solve the underlying least-squares problem for all time steps simultaneously. This amounts to computing  $S_t S_{t-1}^\top (S_{t-1} S_{t-1}^\top + \frac{1}{\lambda} I)^{-1} s_t \quad \forall t$ , a (recursive) least squares solution, where time-shifted (by one) sequence elements play the role of inputs and desired outputs in a dataset, with inputs  $S_{t-1}$ , targets  $S_t$ , and test input  $s_t$ .

With the limited expressivity of one layer, we have already established that Transformers can, and do, in various settings, implement a single gradient step on the corresponding regression problem  $\sum_{t'=1}^{t-1} (s_{t'+1} - W s_{t'})^2$  both in theory and in practice. We now diverge from the previous section which generalized a single mesa-gradient descent step to the multi-layer case. Instead, we argue here that the Transformer could solve the problem differently. Our key observation is that given a preconditioning matrix  $H_t = (S_{t-1} S_{t-1}^\top + \frac{1}{\lambda} I)^{-1}$  which changes the loss as  $\sum_{t'=1}^{t-1} \|s_{t'+1} - W H_t s_{t'}\|^2$ , a gradient descent dynamics would converge in a single step to the regularized least-squares solution. This way, we do not apply several gradient steps, thereby circumventing the potential problems arising from causally-masked gradient descent dynamics on the targets discussed in the previous section.

Based on these insights, we provide a theoretical construction that shows how Transformers can approximate  $(S_{t-1} S_{t-1}^\top + \frac{1}{\lambda} I)^{-1} q_t$  layer by layer in their forward pass, leading to improved single-step gradient descent performance. To do so, we build on the derivations of Section A2.3, where we showed how to implement an approximation of  $\tilde{s}_t := (S_{t-1} S_{t-1}^\top + \frac{1}{\lambda} I)^{-1} s_t$  efficiently, and for all time steps  $t$  in parallel. We achieved this result with the help of the dot-product-attention (DPA) operation at the heart of linear and softmax self-attention layers, and by resorting to the truncated Neumann series.

First, we recall from Section A2.3 that we can approximate  $\tilde{s}_t$  by  $\tilde{s}_t^K$ , obtained when multiplying  $s_t$  to the  $K$ -step truncated Neumann series approximating the inverse term  $(S_{t-1} S_{t-1}^\top + \frac{1}{\lambda} I)^{-1}$ , modulo normalization of the matrix, see A2.3. Then, we observe that the  $\tilde{s}_t^K$  satisfy the following

recursive relationship:

$$\begin{aligned}\tilde{s}_t^{k+1} &= \left( I - (S_{t-1}S_{t-1}^\top + \frac{1}{\lambda}I) \right) \tilde{s}_t^k + s_t \\ &= s_t + \left( 1 - \frac{1}{\lambda} \right) \tilde{s}_t^k - S_{t-1}S_{t-1}^\top \tilde{s}_t^k.\end{aligned}\tag{A44}$$

We now see how, if  $(\tilde{s}_t^k, s_t, s_{t-1})$  is present in the activations at layer  $k$  at time point  $t$ , then  $\tilde{s}_t^{k+1}$  can be computed for the next layer. In particular, the last term in eq A44, can be obtained by

one head of linear self-attention from the input  $(\tilde{s}_t^k, s_t, s_{t-1})$  when  $W_k^\top W_q = \begin{pmatrix} 0 & 0 & 0 \\ 0 & 0 & 0 \\ I_x & 0 & 0 \end{pmatrix}$ , and

$$PW_v = \begin{pmatrix} 0 & 0 & -I_x \\ 0 & 0 & 0 \\ 0 & 0 & 0 \end{pmatrix}.$$

The other terms are simple scaled additions to  $\tilde{s}_t^k$  of  $\tilde{s}_t^k$  itself and  $\tilde{s}_t$

for which many constructions exist. The latter information is also available at all times if not overwritten otherwise. Note that this weight construction strictly speaking only requires 3 channels i.e.  $e_t = (s_t, s_t, s_{t-1})$  in which we update the first by the just provided Neumann series computation. Nevertheless, in practice we still use  $e_t = (0, s_t, s_t, s_{t-1})$ , i.e. tokens with additional memory. We observe in practice that both constructions e.g.  $e_t = (0, 0, s_t, s_{t-1})$  or  $e_t = (0, s_t, s_{t-1})$  reach similar performance but observe more training difficulties and instabilities for the more compact one. We also stress that the derivation presented here is one out of possibly many ways of how Transformers could implement and approximate the desired inverses  $(S_{t-1}S_{t-1}^\top + 1/\lambda I)^{-1}s_t$  in parallel. This is the main reason we resorted to the probing analyses presented in the main text.

## A5 ANALYSING CONTRACTING LINEAR DYNAMICS

We show here the preliminary result when diverging from orthogonal teachers  $W$  to construct the sequence presented to the Transformer and restrict the eigenvalues of  $W \sim \mathcal{N}(0, I)$  in a band of  $[0.9, 0.3]$ . We notice that with these  $W$  approximately 2% of the sequences lead to very large values. To ease trainability, we therefore clip all the values of those sequences to values between  $[-2, 2]$ .

When training a single layer of linear self-attention, see Figure A9, we observe that the trained layer outperforms a naive step of GD dramatically - while the mesa-layer still outperforms both. These findings differ therefore from results obtained when training on an orthogonal teacher. We again find clean weight structure but qualitatively different weights found by optimization compared to weights trained on sequences which are generated by an orthogonal teacher, see Figure A2. We speculate at this point that the meta-learned initialization  $W$  of the model provides a much more favorable initial guess in this setting compared to the orthogonal teacher. Therefore, only *adjusting*, by the residual connection, the current input element of the sequence leads to a large performance boost when compared to naive GD, for which we only tune the learning rate and do not meta-learn an initial model that we update. Nevertheless, we still find gradient descent implemented in the weights even in this setting. We stress that we believe the emergence of gradient-descent-like algorithms will be dependent on the data statistics as well as other experimental design choices (Raventós et al., 2023). We leave this important investigation for future work. We use the same training hyperparameters as when training on orthogonal teachers  $W$ .

## A6 EXPERIMENTAL DETAILS

### A6.1 TRAINING TRANSFORMERS ON LINEAR DYNAMICAL SYSTEMS

We provide here details about the training details of the Transformer models when training on the linear dynamics setting. As described in the main text we focus on fully-observed linear dynamical systems and use a simple generative model. To create a sequence  $s_{1:T}$  we first draw a random ground-truth  $D_s \times D_s$  weight matrix  $W^*$  as well as a random initial state  $s_1 \sim \mathcal{N}(0, I)$ ; the subsequent states for  $t = 2, \dots, T$  are then generated according to the rule  $s_{t+1} = W^*s_t + \epsilon_t$ , where  $\epsilon_t \sim \mathcal{N}(0, \sigma_s^2 I)$  introduces uncorrelated Gaussian noise. We take  $W^*$  to be a random orthogonal matrix. Now, as

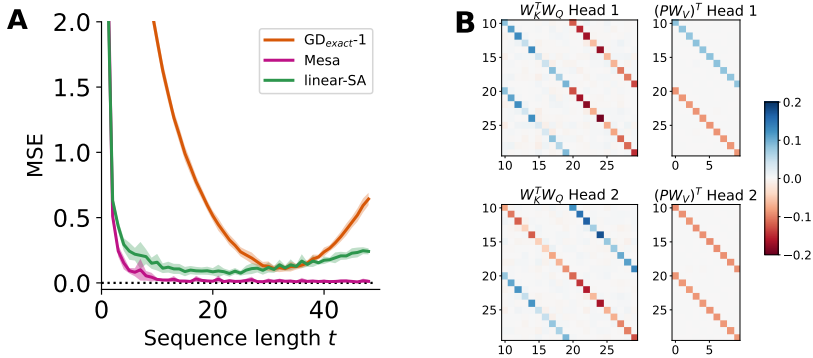


Figure A9: **Training a single linear self-attention layer on contracting linear dynamics** The trained single layer strongly outperforms (A) a naive step GD, diverging from results obtain when training on an orthogonal teacher. We find clear structure in the weights of the trained model (B), as found when training on sequences generated by orthogonal  $W$ , see Figure 2. However, here we see an equal emphasis on all diagonals. Previously, we established a direct link between the weights found in 2 and gradient descent. The predictions of a single layer with these weights are still explained by A42, which includes a gradient-descent term, but here we find similar weight for other non-GD terms in the formula as well, indicating their usefulness in settings different to our original linear sequence models.

already stated we train all Transformer models on the following autoregressive linear regression loss

$$\mathcal{L}(\theta) = \mathbb{E}_x \left[ \frac{1}{2} \sum_{t=1}^{T-1} \|s_{t+1} - f_t(s_{1:t}, \theta)\|^2 \right]. \tag{A45}$$

In all of our experiments, we employ causal masking during self-attention, implemented in the same way as in the majority of auto-regressive language modeling experiments. Specifically, during the self-attention operation we zero out the elements corresponding to the upper triangular matrix of the attention map, except for the diagonal itself. We do this both for the linear attention layer and for the mesa-layer. In practice, for softmax self-attention the incoming logits to the softmax are set to  $-1e^{30}$ . We did not use LayerNorm (Ba et al., 2016) in our models, except for A13, but ran into stability issues especially when training hybrid models with linear layers. To mitigate those, we simply clipped the activations of the forward pass to values between  $[-1, 1]$  which stabilized training significantly. Hyperparameters and other experimental details can be found in table A2.

A6.1.1 SINGLE-LAYER LINEAR SELF-ATTENTION TRANSFORMER

We analyze single-layer, two-head, key-size-20 Transformers, trained on constructed tokens, by comparing their performance with other models and providing an interpolation in parameter space between trained Transformers and the provided construction, which can be described using only a few hyperparameters, see Table A41. While we read out the predictions from the first  $D_s$  entries of the outputs (which initially contain a zero-vector), we simulate a residual connection by manually adding  $s_t$  to the output of the single layer. Since we do not use an embedding layer in this setting, during training we learn another parameter  $\alpha$  as a factor for the added  $s_t$ , such that the prediction reads  $\hat{s}_{t+1} = \alpha \cdot s_t + LSA(e_t; (e_{t'})_{t'=1}^t)$ . For the performance analysis, these models are compared to ‘exact’ gradient descent, a single gradient update step on the auto-regressive loss, and a single mesa-layer. The optimal learning rate for this gradient descent step is line-searched.

**Interpolation details:** We first train a Transformer, then extract scalar parameters, e.g.  $d^{KQ11}$  (see A41), from the  $D_s \times D_s$  sub-matrices by taking the mean of the sub-diagonals of the matrix products  $W_k^T W_q, P W_v$ . We proceed by using these to both build a construction of sparse weight matrices, each consisting only of identity-sub-matrices (scaled by the resp. parameters), and, for the single-layer case, also directly compute a loss for the hard-coded implementation of Table A41 with the respective parameters. Then, during a second training-run of a Transformer for the same initial conditions, we simultaneously compute the test loss for an interpolation, where we average equally

Table A2: Hyperparameters for all settings and model variants when training on simple linear dynamics.

Hyperparameter	Value
Context size	We used length 50, except for the ICL experiments, where we used length 224.
Optimizer	Adam (Kingma & Ba, 2015) with $\epsilon = 1e^{-8}$ , $\beta_1 = 0.9$ , $\beta_2 = 0.999$
Weight decay	0.1 for constructed tokens, 0.05 otherwise
Batchsize	2048 for constructed tokens, 256 otherwise.
Gradient clipping	10 for constructed tokens, 1 otherwise
Activation clipping	Clip $[-5, 5]$ for all models trained on constructed tokens, clip $[-1, 1]$ for hybrid models, no clipping otherwise.
Positional encodings	We add positional encodings of dimension 40 for models trained on unconstructed tokens, otherwise no positional encodings.
Dropout	We do not use Dropout for any model.
Architecture 1-L. Constr.	We use a 1-layer, 2-head, key-size 20, dim-30-tokens, no input- or output-embedding architecture for single-layer models trained on constructed tokens.
Architecture 6-L. Constr.	We use a 6-layer, 4-head, key-size 20, dim-40-token, no input- or output-embedding architecture for the multi-layer models (softmax and linear) trained on constructed tokens for the probing analysis and used key-size 40 for the interpolation.
Architecture 7-L. No Constr.	We use a 7-layer, 4-head, key-size 20, dim-10-tokens, dim-40-embedding- architecture with input- and output-embedding layers for hybrid- and softmax-only-models. Hybrid models contain a softmax and afterwards linear self-attention-layers. The MLP-softmax model contains MLPs with one layer of hidden activations of size 160 and 2 layer- normalization layers (Ba et al., 2016), one directly after the attention layer and one directly after the MLP.
Architecture Hybrid-Mesa	We use 2-layer, 4-head, key-size 20, dim-10-tokens, dim-40-embedding-architecture with inputs- and output embedding layers. First a softmax-self-attention layer, then a single Mesa-layer.
Weight init	$W \sim \mathcal{N}(0, \sigma^2)$ with $\sigma = 0.0002$ for models trained on constructed tokens and $\sigma = 0.05$ for all other models. We always fixed the bias parameters to zero.
Learning rate (scheduler?)	For models trained on non-constructed tokens, we used linear warm-up starting from 0 to $7e^{-4}$ in 500 steps, Cosine annealing to $1e^{-5}$ for the next 20000 steps. We note here that we only train softmax-only and softmax-mlp models for this amount of steps. For models trained on constructed tokens, we never trained for more than 5000 steps. For models trained on constructed tokens, we used a fixed learning rate of $7e^{-4}$ and $9e^{-5}$ for the interpolations.
Mesa regularization $\lambda$	We initialize the learnable regularization parameter $\lambda$ for every mesa-head to 1.

not between the single weight matrices, but between the correct weight-matrix-products per head to obtain a new, interpolated model. The reason for this procedure is the non-uniqueness of weight matrices to obtain the found matrix products. We repeat this procedure for 5 different seeds, train a newly initialized Transformer each time and plot the obtained mean and standard deviation values for the test loss during training.

#### A6.1.2 MULTI-LAYER SELF-ATTENTION TRANSFORMER

For the multi-layer experiments, we use different settings: For the experiments with constructed tokens, we use a 6-layer, no input- or output-embedding layer architecture, while for the other experiments, we use a 1+6-layer architecture with input- and output-embedding layers, where the first layer is always a softmax self-attention layer, while the other 6 Transformer layers are either 6 linear, 6 softmax self-attention layers, or 1 mesa layer (1+1-layer architecture). We found that forward-pass activation clipping after each layer (except for embedding layers) greatly stabilized training.

**Interpolation details:** The interpolation of multi-layer transformers when training on the token construction, we follow the procedure described in the previous subsection, per layer, but extend it to 4-head key-size 40 self-attention layers: We read off the parameters as the mean of the diagonals of the respective  $D_s \times D_s$  sub-matrices of the resulting matrix weight products  $W_k^\top W_q, P W_v$  per

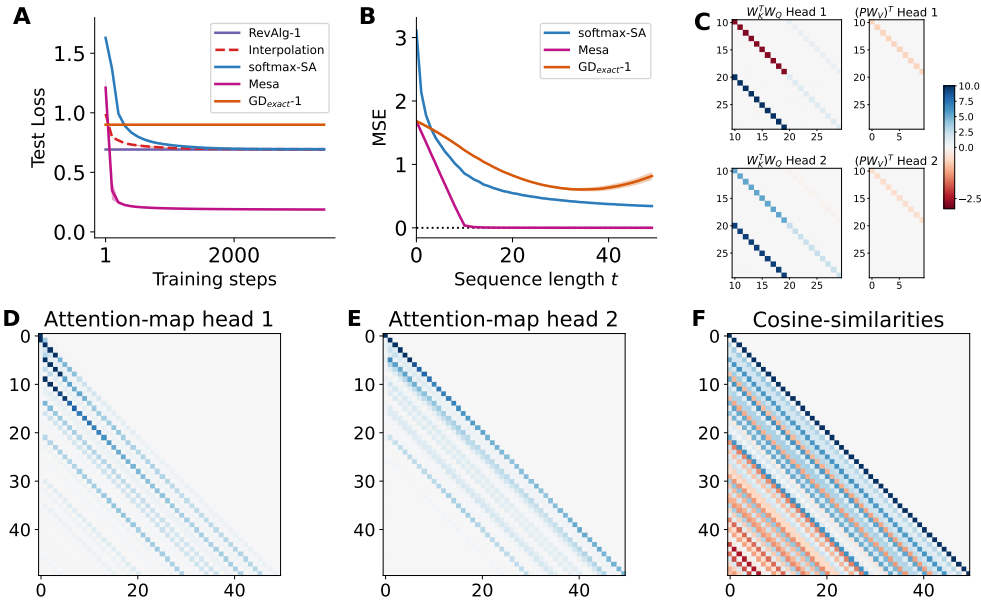


Figure A10: **Reverse-engineering a single trained softmax self-attention layer.** (A & B) The softmax self-attention layer outperforms a plain gradient descent step with the mesa-layer again outperforming both, visible by plotting the loss across the sequence during training (A) as well as when looking at the loss throughout the sequence (B) after training. (C) We show the non-zero parts of the weight-products  $W_K^T W_Q, P W_V^T$  for both heads and find a clear structure as in Figure 2. At this point, we speculate that a mix of gradient descent and induction-head-like copying leads to the final prediction. This is reflected by the softmax attention maps (of a single non-cherry picked sequence) which show waves of attention indicating a copying behavior based on data similarity and not based on positional encodings which are anyway not present here. We again highlight that generally different architectural choices may lead to different mesa-algorithms, here potentially a mix of GD and copying within the model.

head of a trained Transformer. Then we construct sparse weight matrices consisting of identity-submatrices (scaled by the resp. parameters). We use key-size 40 only here as it is otherwise hard to accurately decompose the found weight products into non-square weight matrices. We proceed as for the single-layer experiment and re-train the Transformer from the initial conditions, but during training also report the test loss of a model that is obtained by equally averaging the weight products of our construction and the Transformer. We average the products and not the single weight matrices for the same reasons stated in the previous subsection A6.1.1.

**Probing experiment details:** We presented three variations of probing experiments for the multi-layer models: Target, inverse and implicit target probings. For the basic target probings, we sampled a batch of size 512 and linearly regressed the activations after each layer for that batch against the targets. Using the model learned by the regression, we computed the loss using the same metric as during model training. We repeated this process for 5 different seeds and reported mean and standard deviation in the plotted results.

While analyzing the inverse and the implicit probing experiments, we noticed that a small number of outlier-sequences per batch with had comparably large target norm i.e.  $\|(S_{t-1} S_{t-1}^T + 1/\lambda I)^{-1} s_t\|$ . To overcome this, we introduced a form of dataset pre-processing, where at each token  $s_t$ , we disregarded sequences for which the product  $(S_{t-1} S_{t-1}^T + 1/\lambda I)^{-1} s_t$  with  $z$ -score larger than 2. For the inverse probing, we first pre-process the batch, sorting out  $\leq 5\%$  of the sequences. We proceed now to linearly regress the models activations layer by layer for every time step  $t$  against the implicit targets  $(S_{t-1} S_{t-1}^T + 1/\lambda I)^{-1} s_t$  and report the loss, per token. We tuned the lambda parameter per hand to obtain, across layers, the lowest implicit target probing loss and re-used it for the implicit target probing.

There we proceeded as follows: Per token, we obtained a cleaned batch as in the inverse probing, then computed the products  $(S_{t-1}S_{t-1}^\top + 1/\lambda I)^{-1}s_t$  and  $S_tS_{t-1}^\top$ . We first linearly regress the activations at each layer against the inverse token product as in the inverse probing experiments and obtain a linear model  $W_{t,\text{inverse probe}}^{(d)}$  for every layer and time step  $t$ . Then we multiply the activations at each layer with this learned model per layer and the other product  $S_tS_{t-1}^\top$  to obtain a least-squares prediction model - or when learning a model based on a single gradient descent step. The prediction of this model is weighted with a learning rate which we again tune by hand to achieve overall, across layers, the best implicit target. We define this prediction/vector as  $g_t^{(d)} = \eta S_t S_{t-1} W_{t,\text{inverse probe}}^{(d)} e_t^{(d)}$ , see Figure A12 & A13. Note again that if  $W_{t,\text{inverse probe}}^{(d)} e_t^{(d)} = (S_{t-1}S_{t-1}^\top + 1/\lambda I)^{-1}s_t$  and  $\eta = 1$  we descent the loss optimally well in one step. We compute the loss per token and layer of this prediction model by directly comparing it with the actual targets for one batch. This procedure is repeated for 5 seeds and we report the mean and standard deviation. Furthermore, we include one step of gradient descent as a comparison baseline. To provide a fair comparison between the implicit target probes, we do not compare to  $-\eta S_t S_{t-1} s_t$  i.e. a naive step of GD, for which we obtained much worse results, but use (with abuse of notation)  $\text{GD}_{\text{exact}} - 1 = -\eta S_t S_{t-1} W_{t,\text{inverse probe}}^{(d)} e_t^{(0)}$  i.e. the performance after the data embedding based on the same cleaning procedure. We tuned the learning rate and  $\lambda$  parameters for all settings parameters by hand.

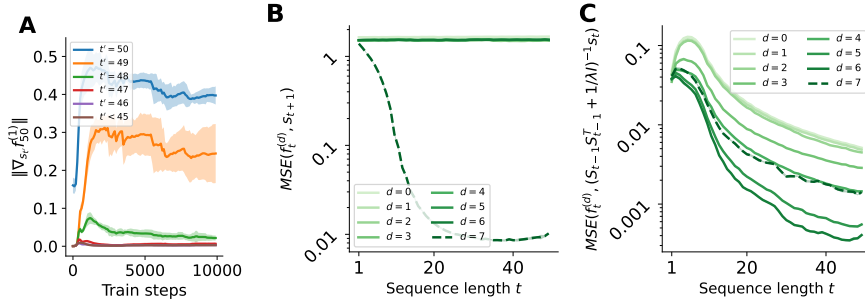


Figure A11: **Reverse-engineering full-fledged Transformers: Linear-Hybrid 1+6-layer model** (A) The first softmax layer groups together neighboring tokens. This can be seen in the high sensitivity to the current and previous tokens of the outputs of the first layer of a hybrid-linear Transformer. (B & C) We linearly regress the activations of each layer against final targets (C) as well as  $(S_{t-1}S_{t-1}^\top + 1/\lambda I)^{-1}s_t$ , the curvature-corrected inputs (D) predicted by the provided theory. We observe a harsh phase transition in the last layer when measuring target probing (B) while observing an intriguingly stable and gradual probing for curvature-corrected inputs (C), except for the last layer, where we hypothesize that the worse probing loss is explained by the computation of the actual predictions. Averages computed over 5 different seeds; shaded area represents standard deviation.

### A6.2 TESTING TRAINED TRANSFORMERS ON FEW-SHOT IN-CONTEXT LEARNING

We provide here details about the *post*-training in-context learning experiment. After training, see Section A6.1 for details, we "prompt" the model with few-shot regression datasets i.e. simply switch from sequences  $[x_1, x_2, \dots, x_{t-1}, x_t]$  where  $x_{t+1} = Wx_t$  and  $x_0 \sim \mathcal{N}(0, I)$  to  $[x_1, y_1, \dots, x_N, y_N]$  where  $y_i = Wx_i$  and all  $x_i \sim \mathcal{N}(0, I)$ . Note that there is no relation between  $y_i, x_{i+1}$  as in the autoregressive case. In both cases we sample  $W$ , if not stated otherwise from the same distribution i.e. as random orthogonal matrices. This results in a sequence length of  $t = 2N$  and  $t = 3N$  when incorporating EOS tokens. Throughout the sequence we measure

$$\mathcal{L}_i = \mathbb{E} \left[ \frac{1}{2} \|y_i - f_{2i-1}(x_i; \{(y_j, x_j)\}_{j=1}^{i-1})\|^2 \right]. \tag{A46}$$

for  $i \geq 2$  depicted e.g. in Figure 5.

For the EOS-token fine-tuning experiments, we initialize a single vector  $\text{EOS} \sim \mathcal{N}(0, I)$  and optimize this single vector on the same loss



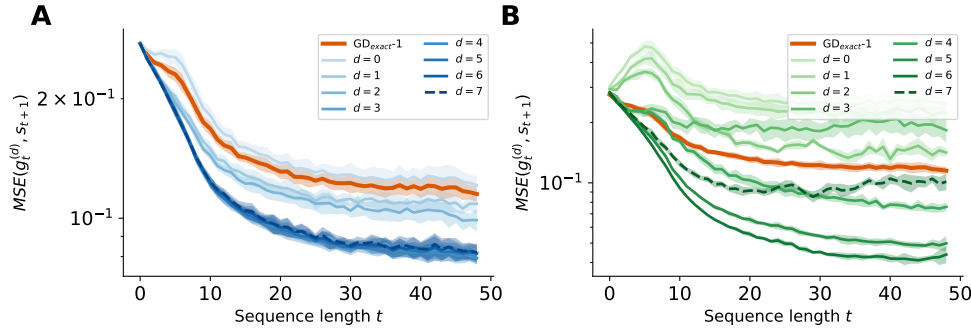


Figure A12: **Implicit target probing for full-fledged Transformers.** To further support the hypothesis that trained multi-layer Transformers first precondition constructed optimization problems by computing an, for example, an approximation of a truncated Neumann series of the required inverses before solving the optimization problems, we provide another probing analysis: For each layer, starting with the embedding layer at  $d = 0$ , we linearly regress the activations against the preconditioned inputs  $(S_{t-1}S_{t-1}^\top + 1/\lambda I)^{-1}s_t$  and multiply these probes with  $\eta S_t S_{t-1}^\top$  to compute a least-squares prediction approximation. We measure therefore measure the possibility to *implicitly* predict the target  $s_{t+1}$  from the hidden activations of the model. **(A)** For full-fledged softmax-only Transformers, we observe as expected, a gradual increase in probing performance across layers as expected at first, where we are able to outperform a step of gradient descent. **(B)** For the hybrid model, we find similar results: The probing performance gradually increases across layers and decreases for the last layer, where we hypothesize that the Transformer performs an update step of gradient descent to solve the well-conditioned optimization problem. Note that again, we are able to outperform a step of gradient descent. Averages computed over 5 different seeds; shaded area represents standard deviation.

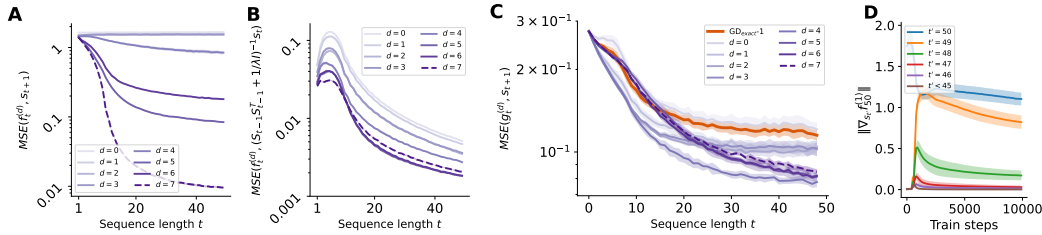


Figure A13: **Probing and copy results for a trained 7-layer Transformer with softmax self-attention layers with MLPs and layer-normalization layers.** Even when training full-fledged Transformers i.e. use all parts of the common Transformer architecture, we observe mostly robust and gradual improved probing on the target and the projected inverse when increasing the sequence as well as the depth. Furthermore, we find very gradually increasing probing results for the implicit target probings as in Figure A12 and especially outperform an update step of gradient descent. In both the inverse and the implicit target probings, we find worse results for the probings of the last layer. We hypothesize the reason for this is the update step on the well-conditioned optimization problem that is performed in the last layer. **(D)** Again, we find very strong copying behavior indicated by the sensitivity analyses.

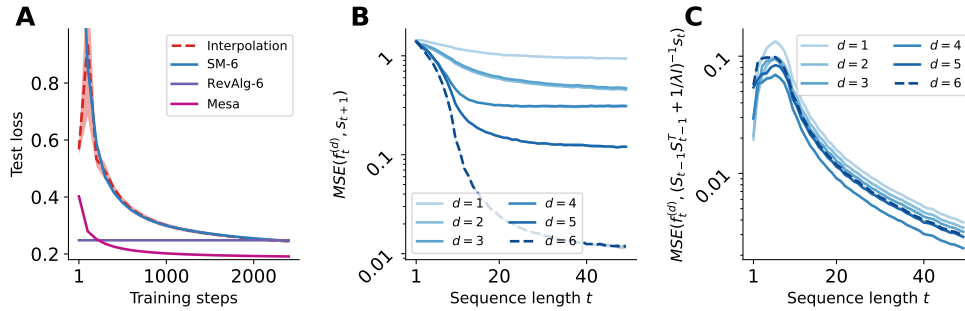


Figure A14: **Reverse-engineering 6-layer softmax self-attention Transformers trained on constructed inputs.** Here we show that a trained multi-layer softmax Transformer trained on constructed tokens is explained by a reverse-engineered algorithm (RevAlg-6) and provide an interpolation between constructed weights and the found Transformer weights. Furthermore, we provide the target as well as inverse probe analogous to Figure 3 and again provide evidence of the hypotheses that targets and the inverse-vector product are gradually approximated throughout depth in the trained Transformer. As the last layer has to perform one update step of gradient descent on the well-conditioned optimization problem, we observe an expected decrease in inverse-probing performance. Averages computed over 5 different seeds; shaded area represents standard deviation.

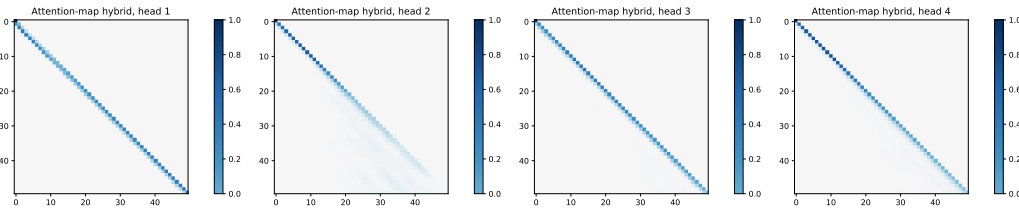


Figure A15: **Softmax attention maps of the first softmax layer when training a linear-hybrid Transformer on unconstructed inputs** We visualize all four heads of the first softmax-attention layer and observe strong copying behavior, as predicted by the provided theory, in the heads i.e. full attention on the current and the previous token. We average the attention maps over a batch of 1000.

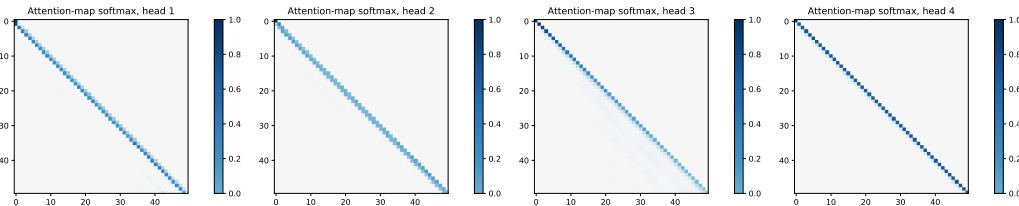


Figure A16: **Softmax attention maps of the first softmax self-attention layer when training a softmax-only Transformer on unconstructed inputs.** We visualize all four heads of the first softmax-attention layer and observe strong copying behavior, as predicted by the provided theory, in the heads i.e. full attention on the current and the previous token. We average the attention maps over a batch of 1000.

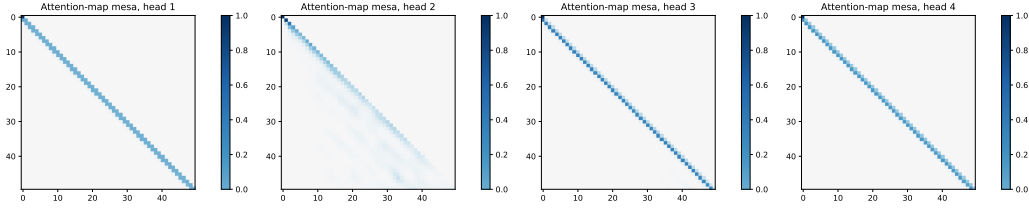


Figure A17: **Softmax attention maps of the first softmax self-attention layer when training a mesa-hybrid Transformer on unconstructed inputs.** We visualize all four heads of the first softmax-attention layer and observe strong copying behavior, as predicted by the provided theory, in the heads i.e. full attention on the current and the previous token. We average the attention maps over a batch of 1000.

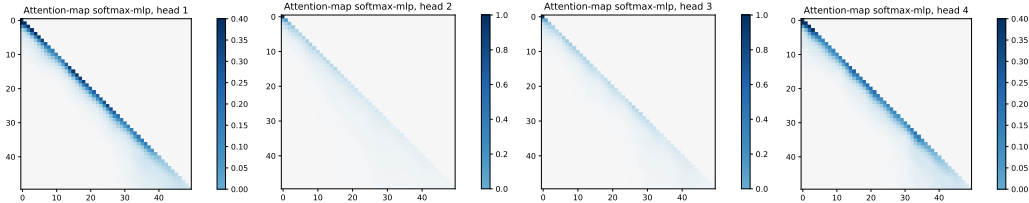


Figure A18: **Softmax attention maps of the first softmax self-attention layer when training a softmax-only Transformer with MLPs and layer-normalization on unconstructed inputs.** We visualize all four heads of the first softmax-attention layer and observe strong copying behavior, as predicted by the provided theory, in the heads i.e. full attention on the current and the previous token. We average the attention maps over a batch of 1000.

$$\mathcal{L}(\text{EOS}) = \mathbb{E} \left[ \frac{1}{2} \sum_{i=1}^N \|y_i - f_{3i-2}(x_i, \text{EOS}; \{(y_j, x_j)\}_{j=1}^{i-1})\|^2 \right] \quad (\text{A47})$$

via batch gradient descent for 100 steps with batchsize 1024 on randomly sampled training data. Note that we interleave every datapair with an EOS token i.e.  $[x_1, y_1, \text{EOS}, x_2, \dots, y_{N-1}, \text{EOS}, x_N, y_N]$  and we therefore increase the sequence length from  $2N$  to  $3N$ .

For the prefix-prompt  $P$ , we fine-tune a single sequence of 20 tokens which we append at the beginning of every in-context learning sequence. We initialize here again all vectors before training of the soft-prompt  $P_i \sim \mathcal{N}(0, I)$  and optimize again the same loss with or without the additional (pre-trained, see above) EOS token

$$\mathcal{L}(P) = \mathbb{E} \left[ \frac{1}{2} \sum_{i=21}^{N-20} \|y_{i-20} - f_{3i-2+20}(x_{i-20}, P, \text{EOS}; \{(y_j, x_j)\}_{j=1}^{i-21})\|^2 \right] \quad (\text{A48})$$

via batch gradient descent for 100 steps with batchsize 1024 on randomly sampled training data resulting in sequences  $[P_1, \dots, P_{20}, x_1, y_1, \text{EOS}, x_2, \dots, y_{N-1}, \text{EOS}, x_N, y_N]$

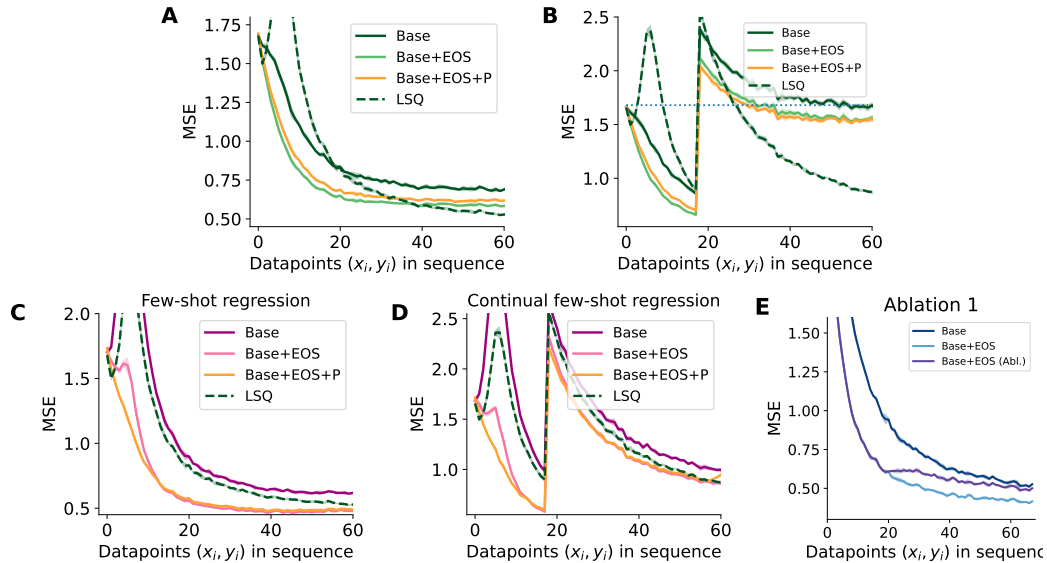


Figure A19: **Autoregressively-trained hybrid-mesa and hybrid linear Transformers prompted to solve supervised few-shot regression problems.** We present here the results analog to Figure 5 in the main text with hybrid-linear (A & B) and hybrid-mesa (C & D) Transformers. The in-context learning performance for both models decreases gradually and significantly with the number of labeled examples. Again, when prompted with a special EOS token or a prefix-prompt P, which we both fine-tune for this regression task on a held-out training set, the performance improves considerably. This highlights the usefulness of prompt-tuning already in this very simple setting. Furthermore, both models show strong performance when tested with multi-task problems, with the hybrid-mesa significantly outperforming the linear model for increasing number of datapoints ( $x_i, y_i$ ). While the hybrid-linear model shows stronger performance for earlier datapoints, the hybrid-mesa model matches (and outperforms) the LSQ baseline with prefix- and EOS-prompting. (E) As an ablation, we test how a softmax-only model, corresponding to Figure 5 of the main text, behaves when tested with a sequence that contains EOS tokens only for the first 20 data pairs. As expected, the performance gradually decreases to non-EOS level once the datapoints are presented without EOS-tokens. Averages computed over 5 different seeds; shaded area represents standard deviation.

Table A3: Hyperparameters for language modelling experiments across all Transformer variants i.e. pure softmax, linear-hybrid and mesa-hybrid with/out MLPs.

Hyperparameter	Value
Dataset	The pile (Gao et al., 2020)
Tokenizer	GPT-2 tokenizer - we append a special "EOS" token between every sequence
Context size	1024
Vocabulary size	50257
Vocabulary dim	756
Optimizer	Adam (Kingma & Ba, 2015) with $\epsilon = 1e^{-8}, \beta_1 = 0.9, \beta_2 = 0.95$
Weight decay	0.1
Batchsize	256
Gradient clipping	Global norm of 1.
Positional encodings	We add standard positional encodings.
Dropout	We use embedding dropout of 0.1 right after adding positional encodings.
Architecture details	12 heads, key size 64, token size 756, no input- but output-embedding
Weight init	$W \sim \mathcal{N}(0, \sigma^2)$ with $\sigma = 0.02$ and bias parameter to zero. We scale all weight matrices before a skip connection with $\frac{1}{2\sqrt{N}}$ with $N$ the number of layers.
Learning rate scheduler	Linear warm-up starting from $1e^{-6}$ to $3e^{-4}$ in the first 8000 training steps, cosine annealing to $2e - 4$ for the next 300 billion tokens
MLP size	Widening factor 4 i.e. hidden dimension $4 * 756$ with ReLU non-linearities (Hahnloser et al., 2000)
Mesa regularization $\lambda$	We initialize the learnable regularization parameter $\lambda$ for every mesa-head to 1.

### A6.3 LANGUAGE MODELING EXPERIMENTS

We provide here details about the language modeling experiments. We use standard values found in the literature and the same hyperparameters, which we did not tune, across all experiments. We, if not stated otherwise, use the standard GPT-2 transformer architecture with LayerNorm (Ba et al., 2016), MLPs between self-attention layer and skip-connection after every layer which we train on a standard (autoregressively) masked cross-entropy loss. We do not use an input embedding layer but an output projection before computing the logits. To train enable stable training of the linear as well as the mesa-layer, we apply the proposed key and query normalization of schlag and simply divide them by their L2 norm. Intriguingly, this stabilizes training drastically also for the mesa-layer after which we did not observe any more instabilities. Note that this is very similar to using additional LayerNorm (Ba et al., 2016) on the keys and queries. Except from this normalization, all models are constructed and trained identically. See A3 for an overview of all design decisions and hyperparameters. Also, we refer to the appendix of Schlag et al. (2021) on how to compute the DFPF kernels to non-linearly alter the key and query features, we use  $\nu = 3$  if not stated otherwise.

## A7 SOFTWARE

The results reported in this paper were produced with open-source software. We used the Python programming language together with the Google JAX (Bradbury et al., 2018) framework, and the NumPy (Harris et al., 2020), Matplotlib (Hunter, 2007), Flax (Heek et al., 2023), Haiku (Hennigan et al., 2020) and Optax (Babuschkin et al., 2020) packages.

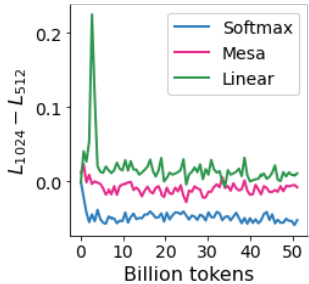


Figure A20: **In-context learning score comparing loss values later in sequence.** When comparing to the in-context learning score comparing earlier time points, Figure 6, we still observe a noticeable gap between mesa and softmax indicating remaining memory retention problems for the mesa-layer. We hypothesize that learned mesa-forgetting factors might close this gap.